A review on nature-inspired gating membranes: From concept to design and applications

Hanieh Bazyar, Othonas A. Moultos and Rob G. H. Lammertink

COLLECTIONS

Paper published as part of the special topic on Fluids Meet Solids

View Online   Export Citation   CrossMark

ARTICLES YOU MAY BE INTERESTED IN

AIP Publishing

A review on nature-inspired gating membranes: From concept to design and applications

View Online Export Citation CrossMark

Hanieh Bazyar,[1,a] (iD) Othonas A. Moultos,[1,a] (iD) and Rob G. H. Lammertink[2,a] (iD)

AFFILIATIONS

[1] Engineering Thermodynamics, Process & Energy Department, Faculty of Mechanical, Maritime and Materials Engineering, Delft University of Technology, Leeghwaterstraat 39, 2628CB Delft, The Netherlands
[2] Department of Science and Technology, Soft Matter, Fluidics and Interfaces (SFI), University of Twente, Enschede, The Netherlands

Note: This paper is part of the JCP Special Topic on Fluids Meets Solids.
[a] Authors to whom correspondence should be addressed: H.Bazyar@tudelft.nl; o.moultos@tudelft.nl; and r.g.h.lammertink@utwente.nl

ABSTRACT

Nature has been a constant source of inspiration for technological developments. Recently, the study of nature-inspired materials has expanded to the micro- and nanoscale, facilitating new breakthroughs in the design of materials with unique properties. Various types of superhydrophobic surfaces inspired by the lotus/rice leaf are examples of nature-inspired surfaces with special wettability properties. A new class of functional surfaces whose design is inspired by the pitcher plant are the slippery liquid-infused porous surfaces (SLIPS). This Review summarizes the properties, design criteria, fabrication strategies, and working mechanisms of both surfaces with specific focus on SLIPS. The applications of SLIPS in the field of membrane technology [slippery liquid-infused membranes (SLIMs)] are also reviewed. These membranes are also known as liquid gating membranes due to the gating functionality of the capillary-stabilized liquid in the membrane pores leading to a smart gating mechanism. Similar to the gating ion channels in biological systems, the pores open and close in response to the ambient stimuli, e.g., pressure, temperature, and ions. Different types of stimuli-responsive smart gating membranes are introduced here, and their properties and applications are reviewed in detail. Finally, challenges and perspectives on both SLIPS and smart gating membranes are discussed. This Review provides a thorough discussion and practical applications of nature-inspired functional surfaces and membranes to pave the way for future research and further developments in this emerging field.

I. INTRODUCTION

Nature has always been the most valuable source of inspiration for human innovations, from technological ideas and engineering to groundbreaking inventions.[1] A field that has largely benefited from natural inspiration is architecture. The constructions by Eiffel, Gaudí, and Paxton are characteristic paradigms inspired by nature. The lotus temple in India, the national stadium in China, and the Olympic pavilion in Barcelona are only a few from the countless examples across the world. However, most of these examples mimic their natural counterpart only in shape but not in function.[2] Discovering the fundamental mechanisms triggering unique biological properties is the key to successful design and fabrication of artificial nature-inspired materials/structures.[3] Such inspirations can be realized in materials, processes, or designs. A detailed overview of nature-inspired materials is given by Katiyar et al.,[4] where examples spanning the laboratory to industrial scale are also reviewed to highlight emerging opportunities. With the developments that have taken place in the field of microengineering/nanoengineering in the last couple of decades, the design and fabrication of nature-inspired materials have been broadened to the microscale/nanoscale. Structures with micro-/nano-features with attractive properties have been developed.[5–8] One of these properties, playing an important role in a broad range of applications, is wettability.[9] The chemical composition of surfaces (defined by the surface free energy) is the main contributing factor affecting the wettability of surfaces. The effect of chemical composition is rather restricted since surface roughness is another key element affecting the wettability of surfaces. As an

example, surfaces with $-CF_3$ functional groups have the lowest free energy and, thus, the highest hydrophobicity. However, the largest contact angle (CA) can reach a value of only ~120°.[10] Extreme wettability phenomena, i.e., superhydrophobicity (CA > 150°) and superhydrophilicity (CA ≈ 0°), are commonly encountered in nature, e.g., in plant leaves and insect wings.[9,11] Surfaces such as lotus and rice leaves,[12–14] butterfly wings,[15] mosquito compound eyes,[16] cicada wings,[17] rose petals,[18] gecko feet,[19,20] and insects (e.g., desert beetle[21] and water striders[22]) exhibit extraordinary superhydrophobicity.

Water droplets normally bounce and roll, instead of stick and slide, on superhydrophobic surfaces since there exists no affinity between water and these surfaces.[23–25] This feature is responsible for the self-cleaning ability of the surface of many plants, including the lotus leaf. In the pioneering work by Neinhuis and Barthlott,[13] the micromorphological characteristics of two hundred plant species with water-repellent properties were investigated. For instance, in lotus leaves, the epidermal (outermost) cells create papillae [see Fig. 1(c)], which provide a microstructural feature/roughness. A hair-like layer, namely, epicuticular waxes (wax tubules), covers the papillae leading to nanostructural roughness[26–28] [see Fig. 1(d)]. Figure 1 shows a lotus leaf and a schematic illustration of its self-cleaning ability as water rolls on the surface, along with scanning electron microscopy (SEM) images of the leaf's upper side at different magnification levels. The micro-/nanostructural roughness, in addition to the hydrophobic nature of the wax tubules, results

in a diminished contact area between water droplets and the surface of the leaf, leading to a static contact angle that is higher than 150° on lotus leaves. Upon tilting the surface (even at low angles), water droplets start rolling off the leaves, removing dirt from the surface, i.e., manifesting a self-cleaning property [see Fig. 1(b)].[29] Due to this ability, the lotus leaf is considered as a "symbol of purity" in a number of Asian belief systems.[13]

Soon after the discovery of superhydrophobic biological materials, efforts were devoted to fabricating artificial bioinspired superhydrophobic surfaces. Different methods, such as the template-based techniques, photolithography, chemical vapor deposition, electrochemical deposition, and phase separation micromolding, have been utilized to fabricate various micro- and nanostructures on a diverse range of materials in an effort to induce superhydrophobicity.[32–36] Superhydrophobicity and other properties thereof stem from the entrapped air between the micro- and nanostructures, which further reduces the area of contact between the water and the solid. Subsequently, this gives rise to CA > 150° with low sliding angles (<10°), making these surfaces ideal for applications requiring self-cleaning,[37,38] liquid-repellency,[38] icophobicity,[39,40] and antifogging[41,42] properties. Superhydrophobic surfaces have been also developed and studied in detail to produce (partial) slip surfaces.[43–48] An overview of experimental and numerical studies of superhydrophobic surfaces for drag reduction purposes (such as in marine environments) is given by Samaha et al.[29] The stability of the air–water interface that is present at a superhydrophobic interface under hydrostatic pressure is a key working parameter. Most of the properties of superhydrophobic surfaces rely on the air cushions trapped between the surface micro-/nanoscale features. However, these surfaces fail to retain this property in the case of low surface tension liquids,[49,50] at extreme environmental conditions such as high humidity,[51] and/or temperatures lower than 0°.[52] The dissolution of air to the surrounding fluid under elevated pressures leads to the failure of such surfaces, especially in submerged applications.[29,53,54] Moreover, for applications involving droplet impact, these surfaces exhibit limited stability[55,56] since the non-wetting properties cannot be maintained for a long time. Such breakdowns are mainly due to the droplet pinning on the micro-/nano-surface structures, leading to a transition in wetting states: from the non-wetting Cassie–Baxter (CB)[57] state to the wetting Wenzel (W)[58] state[59] (see Fig. 2). For more information on the most important theories in the field of wetting and nature-inspired design principles, the reader is referred to the review article by Ashrafi et al.[60] Patterned surfaces with no or minimal tendency toward the CB-W transition can be designed with the help of numerical methods.[61] Pashos et al. showed that the augmented Young–Laplace equation with a pressure term, which accounts for liquid–solid interactions, can aid in solving wetting problems in complex geometries.[62] The minimum energy paths of wetting transitions on pillared surfaces were computed numerically based on the augmented Young–Laplace equation. Using the minimum energy paths, Sheng et al. derived an expression for the calculation of apparent contact angle on structured surfaces.[61] Different categories of surface wettability and the corresponding conditions are studied. Numerical modeling and molecular simulation can be useful tools for studying wetting phenomena, especially in systems that are difficult to realize experimentally.[63–71] Errington and coworkers have performed a series of important studies to compute the
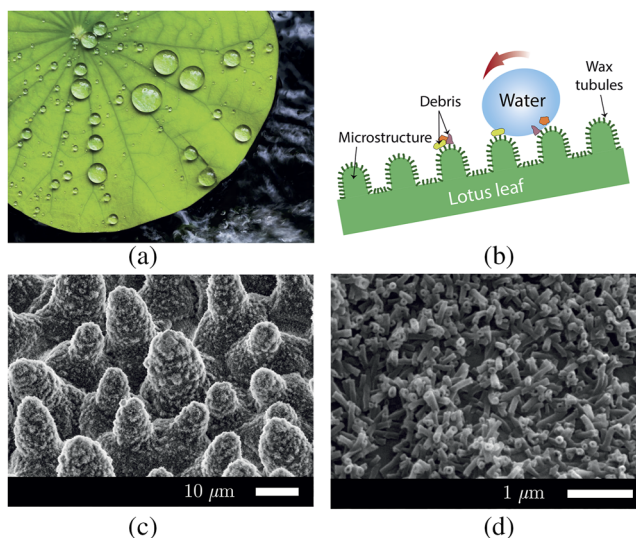
FIG. 1. (a) Photo of a lotus leaf exhibiting extraordinary water repellency on the upper side (adapted from Ref. 30). (b) Schematic illustration of a lotus leaf depicting self-cleaning ability (inspired from Ref. 31). Scanning electron microscopy (SEM) image of (c) the upper side of the leaf showing hierarchical surface structure consisting of papillae, wax clusters, and wax tubules, and (d) wax tubules covering the leaf [figures (c) and (d) are reproduced with modification (addition of the black stripe and change in the text font)] from Ensikat et al., "Superhydrophobicity in perfection: The outstanding properties of the lotus leaf," Beilstein J. Nanotechnol. **2**, 152–161 (2011). Copyright 2011 distributed under the terms of the Creative Commons Attribution 2.0 Generic License, https://creativecommons.org/licenses/by/2.0/.

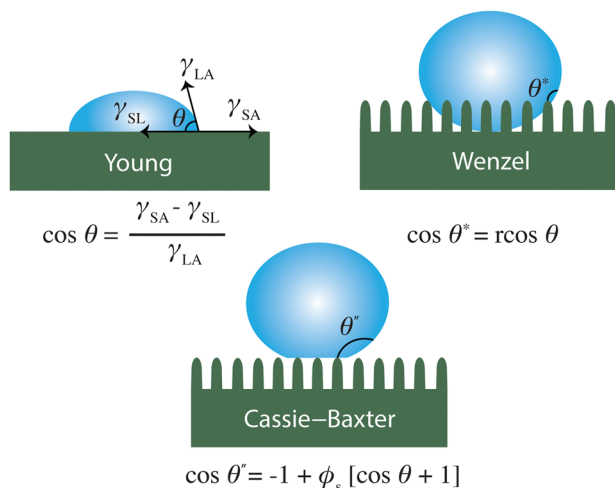**FIG. 2.** Schematic representations of different wetting states of solid surfaces (inspired from Ref. 60) along with the equations that can be used for each state to calculate the contact angle θ. Top left panel: An ideal (smooth and chemically homogeneous) solid surface. The contact angle of a liquid droplet on top of this surface can be calculated using Young's contact angle,[111] where γ_{SA}, γ_{SL}, and γ_{LA} are the solid–air, solid–liquid, and liquid–air interfacial tension, respectively. Top right panel: A rough and chemically homogeneous surface in which liquid penetrates the surface structure. The Wenzel equation[58] can be used in this case, where r is the roughness ratio (the ratio of the total surface area to the projected area of the solid). Bottom panel: Rough and chemically heterogeneous (composite) surface in which liquid sits on top of the surface structures. The Cassie–Baxter equation[57] can be used to obtain θ, where ϕ_s is the area fraction of the solid on the surface.

wetting properties of various types of surfaces and interfacial properties of liquid–liquid systems using molecular simulation.[66,67,72–81] Patel and co-workers have also extensively used molecular simulations for studying surface wetting phenomena.[82–87] For more simulation studies on this subject, the reader is referred to Refs. 88–95 and the review articles by Sethi *et al.*[96] and De Coninck and Blake.[97] Such molecular simulation methods are applicable to a wide range of systems and provide a robust route for predicting and understanding the properties of bulk and interfacial systems.[98–101]

The latest developments in the field of nature-inspired surfaces with special wettability, e.g., superwettability, have laid the foundation for developing materials with multiple dimensions, ranging from dimensionless nanoparticles and 1D fibers to 2D surfaces and 3D integrated substrates.[102] The design principles of such materials along with various examples and different possible wetting states are reviewed in detail by Liu *et al.*[102] Nature creates functional and robust surfaces not only from solids but also from liquids. The shape-adapting insect feet, adjustable and impact-resistant toe pads of tree frogs, optical and antifouling surface of human eyes, and the lubricating interface between the knee bones are intriguing examples.[103] For detailed information on the different kinds of nature-inspired materials/surfaces and their applications, the reader is referred to the recent literature.[4,60,104,105] Recent advances in three types of nature-inspired slippery surfaces (superhydrophobic, superoleophobic, and omniphobic) and the corresponding slippery mechanisms have been lately reviewed by Samaha and Gad-el-Hak.[106]

All these are great sources of inspiration for designing advanced and functional materials, e.g., smart gating membranes. There exist many examples of gating functionality in nature and natural organisms. As an example, plants achieve a balanced condition using stimuli-responsive channels in stomata, which control the exchange of water, gas, and energy with them.[107] A more detailed description about nature-inspired gating functionality is given in Sec. IV. Stimuli-responsive smart gating membranes and their applications in water treatment have also been discussed extensively in recent works.[108–110] Yet, a comprehensive review combining and relating the knowledge of nature-inspired non-wetting surfaces to smart gating membranes is largely lacking. In this Review, the properties, working and design principles, and fabrication methods of surfaces with special wettability are extensively covered. With particular focus on the field of membrane technology, stimuli-responsive smart gating membranes, bioinspired gating functionalities, and their unique features are also reviewed here in detail. Challenges and perspectives for future studies are discussed to set the stage for new developments and stimulate the expansion of their application areas.

II. NATURE-INSPIRED LIQUID-INFUSED SURFACES

Through centuries of evolution, nature itself has created a wide variety of surfaces with non-wetting properties. For example, to address the shortcomings of superhydrophobic surfaces, researchers have been inspired by the carnivorous pitcher plants of the genus *Nepenthes*. This plant catches prey with a pitfall trap that consists of a microstructured slippery surface.[112] Figure 3 shows a photo of a pitcher plant along with SEM images of the different functional zones on its surface. A wettable peristome {a collar-shaped structure that surrounds the pitcher opening [see Fig. 3(a)]} is the home of the main nectaries that attract and trap insects/prey.[113] The surface of the peristome is shielded with anisotropic radial ridges [see Fig. 3(d)] to assist pulling the prey toward the pitcher mouth.[113,114] The peristome is highly wettable due to the capillary action between the microscopic ridges. Owing to the lack of adhesion between the insect feet and the fully wetted peristome, the prey slips into the bottom of the pitcher.[112,113] The upper part of the pitcher wall is covered with a densely packed layer of wax crystals [see Fig. 3(b)].[115] The wax surface is non-wettable possessing microscopic roughness, which simultaneously prevents the formation of a foothold for the insects.[116–120] Moving toward the pitcher bottom in the slippery zone, platelets of the upper wax layer appear and completely cover the lower wax layer [see Fig. 3(c)].[121] The wax regions are lubricated with water, creating a highly slippery surface for the insects. This leads to their fall into the digestive zone of the pitcher consisting of viscoelastic pitcher fluid.[120,122,123]

In 2011, Wong *et al.* at Harvard University took inspiration from the *Nepenthes* pitcher plant and designed the so-called slippery liquid-infused porous surface known as SLIPS.[125] This surface is composed of micro- or nanostructures that are used to enclose an infusion liquid (lubricant) forming the repellent surface[125,126] [Fig. 4 (central image)]. There are three main design criteria to fabricate a stable liquid-infused surface: (1) The infusion liquid and the test liquid should be immiscible, (2) the infusion liquid should completely wet the solid substrate, and (3) the solid substrate should have a higher affinity for the infusion liquid over the
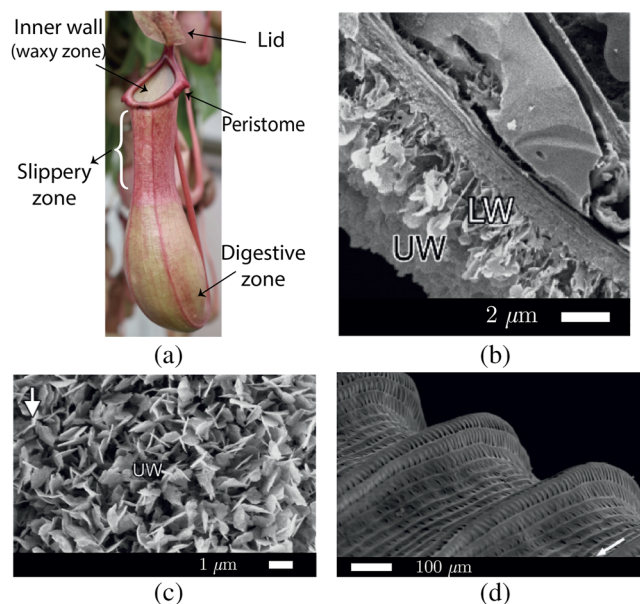
FIG. 3. (a) *Nepenthes* pitcher plant with indicated functional zones (adapted from Ref. 124). SEM images of (b) the wall of the slippery zone's interior showing the wax coverage (LW and UW refer to upper and lower wax, respectively), (c) structure of the upper wax layer [figures (b) and (c) are adapted with permission from E. V. Gorb and S. N. Gorb, "Functional surfaces in the pitcher of the carnivorous plant *Nepenthes alata*: A cryo-sem approach," in *Functional Surfaces in Biology: Adhesion Related Phenomena*, edited by S. N. Gorb (Springer Netherlands, Dordrecht, 2009), Vol. 2, pp. 205–238. Copyright 2009 Springer Netherlands], and (d) peristome surface with first- and second-order radial ridges [adapted with modification from H. F. Bohn and W. Federle, Proc. Natl. Acad. Sci. U. S. A. **101**, 14138–14143 (2004). Copyright 2004 National Academy of Sciences]. Arrows in (c) and (d) indicate the direction toward the inside of the pitcher body.

FIG. 4. Schematic illustration of slippery liquid-infused porous surfaces (SLIPS) (central image) and their key properties (surrounding images).

test liquid.[125,127] The most important design criterion to achieve "liquid-repellency" is criterion (3), i.e., preferential wettability of the solid by the infusion liquid.[125,128] Knowledge of the surface energy of all the present phases is important for choosing the appropriate infusion liquid.[129] The infusion liquid then spontaneously wicks into, and stably adheres within, the substrate by capillary forces.[125] Once this criterion is satisfied, a thin lubricating liquid layer forms on top of the surface, which provides non-wetting and low-hysteresis properties, making the surface "slippery." The resistance to droplet mobility on surfaces is characterized based on contact angle hysteresis (difference between advancing and receding CAs) and the sliding angle (surface inclination to trigger droplet movement).[33] High droplet mobility is obtained on surfaces with high CAs, along with low values of contact angle hysteresis and sliding angle, which is mainly due to the hindrance of pinning.[130,131] This is in compliance with an almost defectless surface stemming from the liquid layer in the case of SLIPS.

Shortly after the introduction of SLIPS, Smith *et al.*[132] performed a fundamental study on the design criteria based on interfacial energy contributions. The physicochemical hydrodynamics upon placing a drop of immiscible liquid on a slippery liquid-infused sur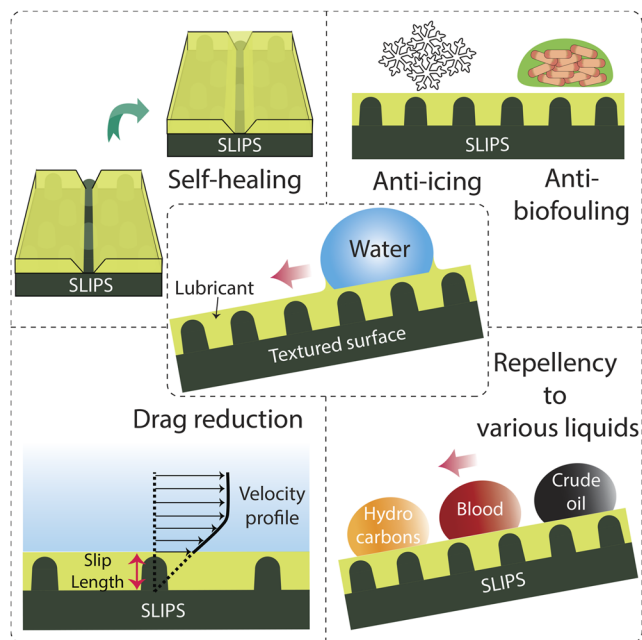face revealed different wetting configurations outside and underneath the drop. It was further shown that drops roll across this surface. The shedding velocity of drops on such surfaces is inversely dependent on the viscosity of the infusion liquid.[133] In an effort to understand the slipperiness and how the infusion liquid alters the static as well as dynamic behaviors of the drop, Schellenberger *et al.* studied the shape of the drop using laser scanning confocal microscopy.[134] This study sheds more light on the main differences between slippery liquid-infused and superhydrophobic surfaces. The differences arise from (1) the formation of a wetting ridge surrounding the drop on the liquid-infused surface and (2) the replacement of air pockets in the superhydrophobic surface with a more viscous and incompressible infusion liquid in the liquid-infused surface. This direct observation further helped measure and estimate the liquid film thickness cloaking the drop. The infusion liquid spreads over and "cloaks" the drop in the case of a positive spreading coefficient $[S_{LD(a)} = \gamma_{DA} - (\gamma_{DL} + \gamma_{LA})]$ in which γ_{DA} is the interfacial tension between the drop and the ambient fluid (e.g., air), γ_{DL} is the interfacial tension between the drop–infusion liquid, and γ_{LA} is that between the infusion liquid–air.[132] The higher interfacial tension of drop–air (γ_{DA}) compared to the summation of that between drop–infusion liquid (γ_{DL}) and infusion liquid–air (γ_{LA}) gives rise to the cloaking of the drop by the infusion liquid. It is important to consider cloaking in the design of a SLIPS since it can lead to gradual loss of the infusion liquid as the drops slide along the surface. It has been demonstrated that this effect should be considered in the design of both macro- and nano-droplets.[135] To obtain more insight into the interfacial phenomena between droplets and slippery surfaces, Pham *et al.* carried out experimental as well as computational studies.[135]

A detailed comparison between superhydrophobic and liquid-infused surfaces in terms of functions and applications was made by Cao et al.[136] and recently by Zeng et al.[105] The advantages and disadvantages of each type of surface are discussed in the work of Cao et al. indicating how to select water-repellent surfaces for practical applications. Liquid-infused surfaces demonstrate remarkable properties ranging from anti-icing,[128,133,137,138] anti-frosting,[137,139] enhanced condensation,[129] and anti-wetting at high temperature[140] to drag reduction,[141–143] self-cleaning,[125,136,144] self-healing by capillary wicking upon damage,[145] antifouling,[146–148] and repellency to various liquids with a vast range of surface tension values[125] (some of these properties are schematically depicted in Fig. 4). In a recent review article by Pakzad et al., the application of SLIPS for drag reduction and the corresponding design criteria along with the challenges for this specific application have been comprehensively detailed.[149] The repellency to a variety of liquids is specifically important in comparison with superhydrophobic surfaces. This further gives rise to applications in the biomedical industry as "paper SLIPS," which can repel liquids with low surface tensions values, e.g., 15 mN/m.[150] With the unique property of "foldability," paper SLIPS can be used for directional transport of liquid droplets due to the easy fabrication of flow channels and switches. The ability of SLIPS to resist most biological fluids leads to a great potential of these surfaces in biomedical applications.[151] In the review paper by Mackie et al., the existing knowledge on the clinical and biological properties of the liquids used in SLIPS along with the developments in understanding the biological interactions of the liquids have been extensively discussed.[152] As mentioned earlier, in superhydrophobic surfaces, contact angle hysteresis increases with decrease in the liquid surface tension, leading to the failure of these surfaces to repel low surface tension liquids.[153] Such a dependence is not observed in SLIPS, thanks to the "physical smoothness" and "chemical homogeneity" of the liquid–liquid interface.[125] Another interesting property of these surfaces is that the optical transparency in the wavelengths corresponds to the visible or near-infrared light.[125,154,155] This requires that SLIPS are engineered in such a way that the chosen infusion liquid and substrate match in refractive indices. In general, maintaining high optical transmittance on surfaces is a challenge in applications, such as in optoelectronics and the automobile and construction industry,[156] due to the accumulation of airborne dust particles. These examples showcase the importance of optically transparent surfaces that are easy and also cost-effective to clean, such as SLIPS. The slipperiness of SLIPS owing to the presence of a smooth liquid layer gives rise to anti-biofouling properties as well.[126,157–159] The mobile character of liquid molecules prevents the formation of a permanent contact between micro-organisms and the surface, thereby significantly perturbing the adhesion between the two and the subsequent biofilm formation.[157,158] Toxicity experiments, using live bacteria species, further confirmed that their anti-biofouling property is not attributed to the toxicity of the infusion liquid.[126,157] With the introduction of stimuli-responsive slippery surfaces with tunable wettability, new application areas, such as droplet manipulation and directional intelligent transportation of liquids, have been investigated.[160,161] Regulations of local wettability via patterned conductive paths can provide individual droplet mobility.[161] A liquid-repellent surface that can switch between SLIPS and superhydrophobic states can be used for programmable fog harvesting.[160]

A. Fabrication of liquid-infused surfaces

As described earlier in Sec. II, substrate surface wettability, governed by surface chemistry and roughness, is an important factor for satisfying the design criteria (2) and (3) of liquid-infused surfaces.[127] Two main approaches to prepare a stable liquid-infused surface consist of (i) proper coating of any rough surface to match the chemical compatibility between the infusion liquid and the solid substrate, and (ii) fabricating a rough, porous, or textured solid substrate from a material with matching chemical compatibility. Depending on the substrate conditions, combination of both methodologies can also be applied.[127,162] While a textured or porous substrate greatly enhances the retention of the infusion liquid compared to flat surfaces (specifically under flow conditions[163]), the chemical compatibility between the two is more vital to guarantee formation of a stable liquid film in liquid-infused surfaces.[127,164] The in-depth argumentation about the design of liquid-infused surfaces, coating methods, and choice of the infusion liquid are elaborated in the review paper by Villegas et al.[127]

Such a film should not be displaced by the impinging test liquid, e.g., water. The infusion liquid must preferentially wet the solid surface. To satisfy this design criterion based on interfacial energy arguments,[132] the summation of the interfacial tension values between solid–infusion liquid (γ_{SL}) and infusion liquid–water (γ_{LW}) must be smaller than that between solid–water (γ_{SW}), leading to a positive spreading coefficient [$S_{LS(W)} = \gamma_{SW} - (\gamma_{SL} + \gamma_{LW})$]. To satisfy this criterion, a solid surface with a low surface energy value, i.e., possessing surface atoms with nearly complete chemical bonds, which is characteristic of hydrophobic surfaces, is required.[156,165] If the solid surface is not hydrophobic by nature, further hydrophobization using low surface tension silane compounds is a possibility. To fulfill the spontaneous imbibition of the infusion liquid into the solid surface as well as complete wetting of the substrate, liquids with low surface tension values such as fluorocarbons (with surface tension ranging between 10 and 20 mN/m[156]) can be used as infusion liquids. The choice of fluorocarbon oils as infusion liquid further satisfies the last design criterion, i.e., immiscibility of the infusion liquid with the majority of impinging test liquids, viz., polar liquids, hydrocarbons, alkanes, etc. Once all these conditions are met, the liquid-repellency of SLIPS becomes insensitive to the solid substrate geometry owing to the presence of a stable lubricating layer covering the surface texture.[125] Various types of oils ranging from alkanes, different types of silicone,[144] and fluorinated oils to ionic liquids[129,132,134,148] can be used as the infusion liquid. The most widely used infusion liquids are silicone[132,136,140,141,166] and fluorinated oils, such as Fluorinert FC70[125,134] and perfluoropolyether (PFPE) with the commercial name of Krytox GPL oils.[125,126,135,137,138,154,155,157,167–169] Using infusion liquids as lubricants has some drawbacks, e.g., volatilization and leakage of the lubricant with long-term usage.[170] Solid phase change materials with inherent lubricant characteristics and thermo-responsive switchable wettability (such as paraffin wax) are promising alternatives.[161,170,171]

Different solid materials and geometries have been used so far to fabricate slippery liquid-infused surfaces. The very first surfaces were made using fluorinated acrylate textured materials[144] and silane-treated periodically ordered/random arrays of nanoposts.[125] The fabrication includes a two-step soft lithography process using epoxy resin.[172] This technique was later

used to replicate the surface microstructures of the taro plant leaf using polydimethylsiloxane (PDMS).[173] Photolithography with deep reactive ion etching was used as an alternative method to fabricate micropost/pillar arrays in silicon.[129,132,157,168,169] The silicon surface was further hydrophobized using silane compounds such as octadecyltrichlorosilane (OTS)[129,132,169] or (tridecafluoro-1,1,2,2-tetrahydrooctyl)-1-trichlorosilane (TFTS).[168] Cylindrical micropillar arrays were also fabricated in glass using photolithographic techniques and etching followed by further silane treatment.[134] Another technique involves using polished silicon wafers that are subjected to a laser ablation process in order to obtain post-like structures having twofold micro- and nano-features.[141] The surface is further silane-treated with OTS while the lubricating oil is later added using the dip coating method.

Most of the recent research works have focused on the fabrication of SLIPS using industrially relevant materials such as metals. Aluminum, as the most widely used lightweight structural material, was electro-polished and subsequently anodized to obtain aluminum oxide layers with pore-like and aggregated pillar-like microstructures.[126] Dipping aluminum in sodium hydroxide solution followed by etching in hydrochloric acid can lead to the formation of $Al(OH)_3$ hierarchical micro-/nanostructures on the aluminum surface.[174] Etching in hydrochloric acid followed by treatment in boiling water is another method to achieve hierarchical structures consisting of nanoflakes on aluminum substrates.[175] Hydrophobization using (1H,1H,2H,2H-perfluorooctyl)-1-trichlorosilane (FOTS) rendered the surface hydrophobic and suitable for liquid infusion. Sandblasting and boehmite treatment of aluminum are other alternative methods.[138] Micro- and nanoscale textures, stemming from sandblasting and boehmite formation, respectively, give rise to hierarchical aluminum structures. Further surface treatment using fluorinated compounds makes the surface hydrophobic and applicable to SLIPS. Stainless steel, the most widely used industrial material, was studied as the substrate of SLIPS as well. It was chemically etched to produce the requisite rough surface structure.[140] Further cleaning and silane treatment using OTS were performed to obtain the hydrophobic surface for infusion of the liquid. Food grade stainless steel and carbon steel were also investigated as substrates of SLIPS.[147,176] To texture the surface, femtosecond laser ablation and nanosecond laser treatment were used, respectively. Further fluorosilanization and impregnation with the perfluorinated oil led to the fabrication of SLIPS. Commercially available oxygen-free copper tubes were also used as a metal substrate.[168] Nanostructured CuO films (sharp, knife-like CuO structures) were obtained on the surface using an oxidation and re-oxidation process. TFTS-silane treatment was subsequently applied to coat the surface. Titanium alloys with excellent corrosion resistance are widely used in the marine industry. Wang *et al.* fabricated nanostructured titanium alloys through anodic oxidation.[146] Subsequent silane treatment followed by infusion with the fluorinated oil provided SLIPS with antifouling properties. Commercial copper foils have also been used as the substrate of SLIPS.[177] Alkali assisted oxidation process was used to form $Cu(OH)_2$ nanowires on the surface of the foils. To obtain durable SLIPS, Cu-based metal–organic frameworks (MOFs) were grown on $Cu(OH)_2$ nanowires, forming a hierarchical structure. PDMS was chosen as the lubricant.

Instead of texturing the solid substrate itself, coating of a structured and rough layer on the substrate is another alternative.

This makes fabrication of SLIPS directly possible on commercially available materials/surfaces. Kim *et al.* used aluminum as the substrate on which nanostructured polypyrrole was electrochemically coated[137] using an electropolymerization technique.[178,179] SLIPS was also fabricated by Long *et al.* on magnesium alloy via spraying a suspension consisting of natural attapulgite (APT) with existing micro/nanoporous structures.[180] After complete curing of the coating, silicone oil was added as the lubricating liquid. Cao *et al.* coated glass with a superhydrophobic mesh using a dip coating process into a PDMS solution.[136] Spray coating/depositing is another versatile method that can be applied to a variety of substrate materials. Spray-depositing of carbon nanofibers (CNFs) dispersed in a fluoroacrylic copolymer on glass was studied by Elsharkawy *et al.*[139] The copolymer solution acts as the low surface energy material (offering the required hydrophobicity) while CNFs provide hierarchical micro-/nanostructures. A commercially available aerosol solution (functionalized silica nanoparticles suspended in a propanol/liquefied petroleum gas mixture) was spray-coated on glass to make superhydrophobic surface possessing a fractal-like porous network. Upon dip coating of the surface in the infusion liquid, SLIPS can be obtained.[166] Sol–gel techniques have also been used as another coating method. Flower-like nano-textured alumina sol–gel coatings were introduced by Ma *et al.*[155] This coating can be applied on various materials (irrespective of the shape) ranging from silicon and glass to metals and even plastics. Further functionalization using perfluorinated compounds and phosphonic acid was performed to render the film surface hydrophobic and suitable for SLIPS. Considering the environmental concerns about fluorinated compounds, silicone-based chemistry has recently attracted more attention as an environmentally friendly alternative.[181] Polydimethylsiloxanes (PDMSs) when grafted on a substrate by UV light or heating serve both as reducing surface energy agent and as lubricating oil, leading to a one-step fabrication process of lubricant-immobilized slippery surfaces.[181–183] This procedure can be applied on any type of substrate, ranging from nonhydrophobic metals and metal oxides to ceramics with various surface morphologies or even nonporous/textured structures. Mussel-inspired chemistry of polydopamine (PDA) is another material-independent coating strategy considering the possibility of PDA to bind to different surface materials.[184] Cofunctionalizing the coating with monoaminopropyl-PDMS adheres silicone polymer chains to any desired surface material. The addition of inert silicone oil to the reaction mixture further provides *in situ* lubrication of the coating. Ecofriendly bio-lubricants based on oleic acid (OA) and methyl oleate (MO) have been investigated as the infusion liquid in UV-treated PDMS substrates for marine applications.[159]

For more flexible substrates, various types of mesh structures have been investigated. Random networks of polytetrafluoroethylene (PTFE) (Teflon) nanofibers create a hydrophobic mesh, eliminating the need for hydrophobization.[125] Spray-coated stainless steel meshes, using aerosol solution, allow for the flow of the infusion liquid between two sides, providing double-sided flexible conformable meshes.[166] Porous architectures with periodically interconnected spherical pores known as inverse opals (IOs) were also studied as substrates for SLIPS.[134,135] Schellenburger *et al.* obtained IOs by vertically lifting a glass substrate out of an aqueous dispersion of polystyrene particles and silica nanoparticles.[134] The polystyrene template was then removed via annealing and

the surface was cleaned and hydrophobized. A gold-coated silicone substrate was studied by Pham *et al.*, which was vertically placed in a well containing colloidal suspension of monodispersed polystyrene spheres.[135] The suspension formed by the colloidal crystal evaporates in the ambient environment followed by further annealing at 95 °C for 3 h. The oval template was removed via immersing in tetrahydrofuran for a minimum of 12 h, revealing an IO structure with an interconnected pore network. After IO fabrication, further dispersion of Krytox GPL oil onto the sample, allowed slow permeation of lubricant through the porous structure.

III. LIQUID-INFUSED SURFACES WITH MEMBRANE FUNCTIONALITY

Examples of fabrication methods for liquid-infused surfaces include complex, time-consuming, two-step soft photolithography processes,[128,172,173] lengthy and expensive photolithography based on deep reactive ion etching processes,[129,132,134,168,169] and chemical etching[140,168] and anodization of metals.[126] Coating techniques provide a more cost-effective and simpler SLIPS fabrication process, involving alumina sol–gel,[155] spray coating,[139,166] electrolytic polymerization of conductive polymers,[137] and dip coating.[136] Yet, all these processes require an extra step for the reduction of surface energy based mostly on silane treatment methods, which increases the cost and fabrication time.

Porous surfaces, such as polymeric porous membranes, are examples of surfaces that provide the required rough and textured solid substrate to contain the infusion liquid without complex and time-consuming fabrication processes.[125,167] Thanks to the wide availability of porous polymeric membranes, including high-fluorine content polymers with intrinsic low surface energy and hydrophobicity, silane treatment is not required. Examples of such polymers are PTFE,[157,167] polypropylene (PP),[167] polyvinylidene fluoride (PVDF),[154,167,185–187] and polyamides (nylon).[154,157,167] The porous structure of such membranes, with pore sizes ranging from micrometers[167] to nanometers,[154,157] can lock the infusion liquid in. Low surface tension infusion liquids, such as silicone oil or fluorinated Krytox, spontaneously infiltrate through the porous structure as a result of capillary wicking, forming a smooth liquid layer on the surface. The low surface energy of the polymer material further ensures that the most important design criterion is met, i.e., preferential wettability of the solid substrate by the infusion liquid relative to an immiscible ambient fluid such as water. Figure 5 illustrates the fabrication steps of liquid-infused surfaces using a porous membrane. The application of polymeric hydrophobic porous membranes as the solid substrate provides a facile, fast, and cheap method to fabricate liquid-infused surfaces with gating functionality, which was first proposed by Hou *et al.* in 2015.[167] This leads to a new class of membranes known as "slippery liquid-infused membranes (SLIMs)" upon addition of the infusion liquid.[186] A systematic overview of the design, properties, and advantages of porous membranes as the substrate of liquid-infused surfaces is given in the work of Wang *et al.*[188]

Similar to liquid-infused surfaces, liquid-infused membranes possess interesting surface properties, e.g., slipperiness, self-cleaning, self-healing, due to the lubricating liquid layer. Owing to these characteristics, liquid-infused membranes demonstrate unique
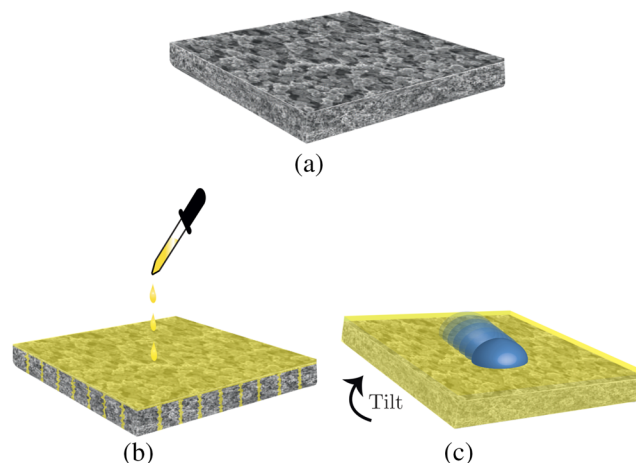

FIG. 5. Fabrication steps of SLIM. (a) SEM images of top and cross section of the PVDF membrane used to construct a 3D view of the membrane. (b) Addition of fluorinated Krytox 101 oil to the membrane. (c) Fabricated SLIM with a smooth lubrication layer showing slippery character.

functions and properties for separation applications. The capillary-stabilized liquid in the membrane pores causes the formation of a pressure-responsive reconfigurable gate (which can close or open depending on the external pressure).[167] Due to this unique gating function, these membranes belong to the category of "smart membranes" with tunable selectivity and/or adaptive surface.[189] The properties of such membranes can be controlled by external stimuli, leading to the design of the so-called stimuli-responsive membranes.[190,191] The external stimuli modulating membrane performance usually falls into the following categories: (i) direct, (ii) indirect, and (iii) field-responsive[190] stimuli. In direct stimulation, the membrane comes directly in contact with chemical/biological stimuli, such as pH changes,[192,193] electrostatic environment, and chemical/biological agents.[190] Indirect stimuli involve incorporating sites (specific chemical groups) on the membrane that are responsive to the temperature or pressure of the environment.[194,195] Other groups can be responsive to pressure and, therefore, to ultrasound. Such membranes are fabricated with smart polymers that can change their morphology on application of ultrasound at a particular frequency.[196] Finally, membranes that are field-responsive can sense external electromagnetic fields. In this case, to elicit a response, no mass/heat transfer between membranes and/or cues is required.[190,197]

IV. SMART GATING MEMBRANE SYSTEMS

The gating function of a membrane mimics the functionality of biological systems in nature, e.g., electric discharges in the electric eel or smell perception in human body.[198] The electric eel can generate considerable bioelectricity (up to 600 V) from the ionic (salt) content in fluids, utilizing ion channels that are highly selective and rectified.[199] The biological ion channels are membrane protein complexes (asymmetric "subnanoscale" protein) with various responsive conformational changes that can regulate fast ion transport with high selectivity[199,200] [Fig. 6 (central image)]. The
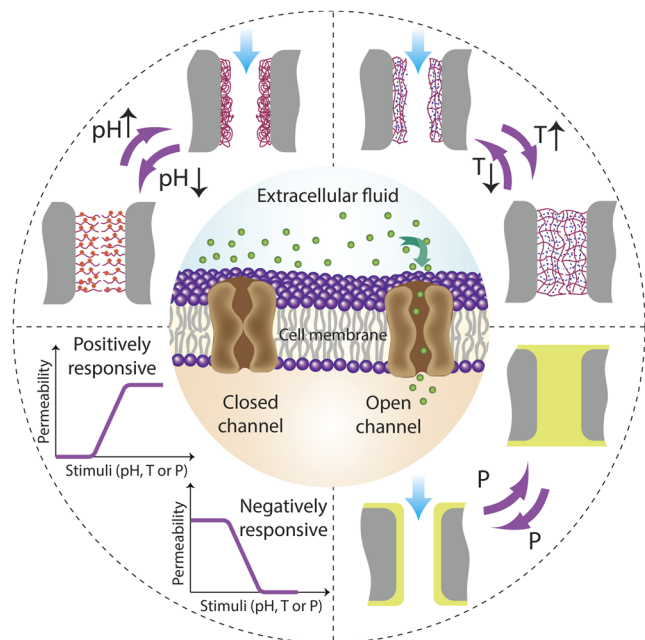
FIG. 6. Smart gating membranes inspired by cell membranes with ion channel [middle (inspired by Ref. 225)] and positively/negatively responsive gating functionality (bottom left). Positively pH-responsive gates (top left). Negatively temperature-responsive gates (top right). Positively pressure-responsive liquid gates (bottom right).

transport of ions in these channels is primarily regulated by three different characteristic mechanisms: (i) ionic selectivity, (ii) ionic rectification, and (iii) ionic gating. In particular, the ionic gating mechanism allows for the channels to open and close (depending on the external stimuli) to regulate the permeation of ions through cell membranes, which are important for sustaining physiological functions in living organisms.[201] For instance, in the open state, ions are allowed to pass through the channel and, thus, electric current is conducted. In contrast, when the gate is closed, no ionic transport is facilitated and, therefore, no electrical current is conducted (voltage sensing capability).[200,202] The liquid gating functionality in a capillary-stabilized liquid-filled pore is inspired by that of their natural counterparts. The microscale xylem and stomata in plants regulate air, water, and microbe transport using liquid-based reconfigurable gates.[203,204] The micropores between alveoli (tiny air sacs) in the lungs are filled with liquid with gating functionality.[167] Upon opening/closing in response to the air pressure gradients, a liquid-lined pore is established. The efficiency of gas exchange in the lungs highly depends on the amount of liquid lining the pore walls.[205] The gating mechanism in biological ion channels (nanopores) has been studied via molecular dynamic (MD) simulations by Dzubiella et al. The MD simulations provide a powerful tool to investigate the water structure in the channels under the influence of the electric field induced by the large ionic concentration gradient. The nanopore that is initially not permeable to water can let water molecules in due to the presence of the strong electric field. The subsequent passage of cations leads to a reduction in the electric field and, thus, closes the pore for further transport of ions.[206] To further study the transport

of ions and water molecules through channels of biological membranes, Yao et al. investigated "carbon nanotube porins (CNTPs)," which exhibit biocompatibility.[207] Gating functionality under the influence of affecting parameters, namely, external voltage at various flow values through the tubes as well as different compositions of the lipid layer, have been studied in depth using continuum modeling. Another example are the external odorant molecules, which act as stimuli to specific ion channels in the human nose system, leading to smell perception in the open state.[198] For detailed information on the olfaction machinery, the transduction mechanism, and theories describing the perception of odor, the reader is referred to the review article by Sharma et al.[208]

Mass transport through membranes can also occur in a "passive" way due to a driving force caused by a gradient in the chemical or electric potential or in the composition across the membrane.[209] Based on their porous morphology, membranes can be divided into homogeneous and heterogeneous structures.[210] Generally, membrane-based mass transfer and separation manifest fantastic characteristics, including a low degree of energy consumption during membrane processes, together with the compactly structured and less space-occupied membrane equipment.[209,211] Consequently, membrane technology is essential with regard to worldwide sustainable development in various respects ranging from conservancy and renewal of energy,[212] decrease in pollutant discharges,[213] to water and wastewater treatment.[214] Despite all the advantages offered by membrane technology, it suffers considerable disadvantages (e.g., the unalterable surface and pore properties) restricting the efficient implementation of membranes in various practical applications.[108] For example, membrane performance is seriously affected by the so-called membrane fouling phenomenon, which is the undesirable accumulation of foulants on the membrane during a separation process. Another example is the limited applicability of membranes in processes/applications that require self-regulated permeability and/or selectivity.[108] Smart or intelligent membranes possessing self-adjustable permeability and selectivity properties should be developed, which will bring new opportunities for broader membrane utilization.[215] In an effort to overcome the limitations and drawbacks of the traditional membrane technologies, smart stimuli-responsive gating membranes have been developed. These artificial membranes are inspired by natural cell membranes with ion channels and are fabricated by incorporating stimuli-responsive species acting as functional gates into traditional porous membranes.[108]

In membranes with functional (smart) gates (switching ability between open and close states), the permeability and selectivity can be self-regulated to respond to the presence of stimuli. The self-regulation of permeability and selectivity can be achieved via flexible alteration of surface properties as well as the pore sizes. This further enables successive separation of multiple components, controlled release, and antifouling and self-cleaning membranes, which have a great potential application in biomedical devices.[216]

A. Design and fabrication scheme

The design and fabrication of smart gating membrane systems are possible via various methods in which the membrane type, gating style, and gate location can be varied.[215] Stimuli-responsive membranes have been employed in the form of flat sheets for

separation,[217] hollow fibers for water treatment,[218] and capsules for controlled release[219] purposes. The gating style highly depends on the type of functional material/molecule used for functionalization of the membrane based on physicochemical modification methods (Fig. 7). The functional gate can consist of linear polymer chains,[220] cross-linked hydrogel networks,[221] or microspheres,[218] which enables shifting between swollen and shrunk states upon the presence of stimuli to adjust the surface characteristics as well as the pore size. The gating material can be integrated at different locations, i.e., into the membrane pores (pore-filling form) or on top of the membrane (pore-covering form). The pore-filling form provides a robust gating performance,[222] while the pore-covering form is useful for applications where rapid response is required.[223] The latter method can get to both sides of the membrane surface with or without full coverage of the pore.[224]

Depending on whether the gate materials (materials inducing gating functionality) are added to the membranes during or after the membrane formation, the fabrication methods of smart gating membranes can be divided into two categories.[108] Integrating gate materials on the existing membrane substrates leads to stimuli-responsive gates that are formed after the membrane production. This can be achieved via grafting-from or grafting-to methods. In the "grafting-from" method, active sites comprising functional monomers are introduced on the surface of the pores, which form linear polymers or cross-linked networks upon polymerization.[221,222] Various grafting techniques, such as plasma-induced grafting,[217,226] chemical grafting,[227] and UV-induced grafting,[228] can be employed for incorporating functional gates into membranes. In the "grafting-to" method, preformed functional materials (polymer chains or microspheres) are chemically/physically incorporated on the surface of membrane pores comprising pretreated active sites.[218,220] The microstructure of the gates can be controlled in a flexible manner using this method. The type of bond between the gate material and the surface of the pore consists of physical interactions, such as van der Waals forces[218] or chemical bonds (for more robust applications).[220] Direct utilization of functional materials for membrane fabrication is the most straightforward method to prepare smart gating membranes and it does not require further modifications.[191] Despite the great potential of this technique for easy scale-up as well as efficient industrial manufacturing of gating membranes, it has been hindered due to the limited options of functional material for membrane fabrication. An alternative approach has been introduced that can be realized by blending the stimuli-responsive materials (block copolymer or microspheres) with the polymer forming the membrane matrix during membrane fabrication.[229,230] Functionalization of membrane pores to obtain smart gating membranes can be realized via various physicochemical modification methods, such as atom transfer radical polymerization,[229] electroless deposition,[231] plasma modification,[232] and self-assembly.[233] These methods are sophisticated, time-consuming, and, in some cases, expensive and not easy to access. As an easy and straightforward method, infusing the membrane pores with an infusion liquid (see Fig. 7 and Sec. III) can provide an alternative approach to obtain reconfigurable gates. This will be discussed further in Sec. IV.

B. Gating functionality

Membrane gating can be divided into two models: positively responsive gating and negatively responsive gating.[108,234] Positively responsive gating allows increased membrane permeability through opening membrane pores in the presence or increase of the stimuli. In sharp contrast, in negatively responsive gating, a large decrease in the membrane permeability occurs due to closure of the membrane pores when external stimuli are present or increase.[108] A schematic representation of these two mechanisms is shown in Fig. 6. A broad range of stimuli can be used to achieve stimuli-responsive gating. Temperature and pH are the most studied stimuli since temperature fluctuations occur naturally in many environmental systems and temperature is well controlled in artificial designs, while pH is a crucial parameter especially for engineering biomedical applications.[234,235] Other types of stimuli that can be considered are ions, e.g., potassium (K^+), which is a key species for biological metabolism.[236] Molecules such as glucose, the concentration of which is an important indicator of, for instance, diabetes in blood, are also promising candidates for further exploration.[237,238] (UV) light, magnetic fields, and ultrasound are "clean" frequently used stimuli that can be utilized for remote control.[196,239,240] The gating functions are manifested via shrinking and/or swelling transitions in stimuli-responsive materials, which can open or close the pores of membranes to tune (increase or decrease) their permeability. Similarly, pore surface properties can be tuned by the hydrophobic or hydrophilic changes related to the transitions of particular types of gates.[215] Another sort of transition in wetting states is known as "dewetting transition." This transition is of great importance in nanopores, leading to a dry state of the pores that are open physically yet not permeable to ions. This interesting phenomenon is known as "hydrophobic gating," which is also utilized by biological protein ion channels for the corresponding regulation of substances. Direct observation of hydrophobic dewetting is still a challenge. In a review article by Yazdani et al., the relevant simulation, theoretical, and
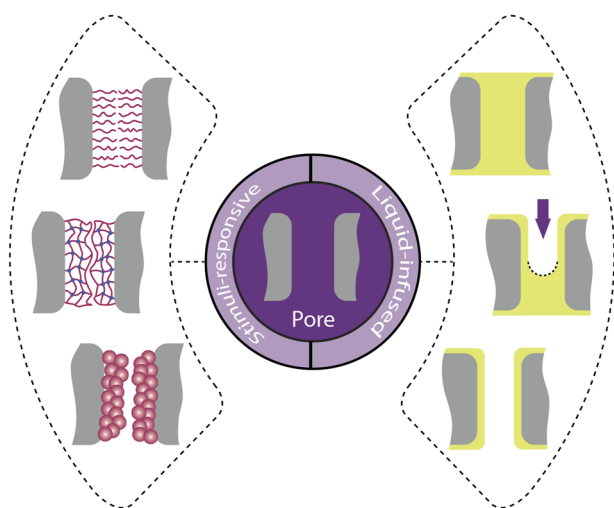

FIG. 7. Smart gating membranes that can be designed either based on the infusion of the membrane pores with a liquid (right) or incorporation of a functional material into the membrane pores (left). This functional group can consist of polymer chains (top), hydrogel network (middle), or microspheres (bottom).

experimental studies have been detailed.[241] As the most common parameters, the fabrication and applications of temperature- and pH-responsive gating will be discussed briefly here. More detailed information on other types of stimuli-responsive gates can be found elsewhere.[108,215]

Poly(N-isopropylacrylamide) (PNIPAM) is a widely used thermo-responsive material in positively responsive gates.[234] PNIPAM undergoes a reversible phase transition at the lower critical solution temperature (LCST) of ~32 °C, which is close to the normal human body temperature.[242,243] At temperatures lower than the LCST, PNIPAM becomes hydrophilic and swells (due to the formation of amide–water hydrogen bonds), causing the membrane pores to close. In contrast, for temperatures higher than the LCST, PNIPAM becomes hydrophobic and shrinks (due to the depletion of hydrogen bonds with the solvent), causing the membrane pores to open (positively thermo-responsive gates).[244] It is important to note that by chemically modifying the PNIPAM chains, using hydrophobic or hydrophilic groups, the desired LCST for specific applications can be achieved. Polymers such as poly(acryl amide) (PAAm) and poly(acrylic acid) PAAc, which form interpenetrating networks (IPNs), can be utilized for the fabrication of negatively thermo-responsive gates. The formation of PAAm/PAAc complexes (due to hydrogen bonding) at temperatures lower than the upper critical solution temperature (UCST) of the IPNs causes the shrinkage of the polymeric gates, which results in open pores and, thus, increase in the membrane permeability. At temperatures higher than the UCST, hydrogen bonds are depleted, causing the dissociation of the IPNs. This is manifested by the swelling of IPNs, which, in turn, leads to closed membrane pores (decrease in permeability). In short, by controlling the temperature to lie above or below the UCST, the membrane pores can be switched "on" or "off."[221] Inspired by the plant stomata, Ding *et al.*[195] recently developed a smart thermo-responsive wood-based membrane (reversible open/close function of the pores upon heating/cooling cycles). This was achieved by polymerizing the PNIPAM inside the scaffold of the wood at a temperature higher than the LCST, producing a hydrogel with heterogeneous microstructure.

The mechanism causing materials to be pH-responsive (e.g., pH-induced swelling or shrinking) is based on the presence of acidic and basic groups. These groups gain or lose protons based on the pH level of the environment.[245] For example, it is shown that poly(methacrylic acid) (PMAA) and poly(N,N-dimethylaminoethyl methacrylate) (PDM) hydrogels undergo pH-induced volume phase transitions of opposite nature.[246] In particular, hydrogens produced from PMAA exhibit a positively pH-induced volume phase transition. This is manifested by the swelling of the PMAA chains when the environmental pH increases. In sharp contrast, hydrogels produced from PDM are shown to undergo a negatively pH-induced volume phase transition, which is manifested by the swelling of the polymeric chains when the environmental pH decreases. Therefore, PMAA (or PAAc) is used as a negatively pH-responsive model[246,247] for smart gating membranes and PDM as a positively pH-responsive model.[229] Recently, pH-responsive polymers have been utilized for membrane fabrication via novel and sustainable aqueous phase separation techniques.[193] As expected, pH-responsive polymers are used to design pH-responsive membranes. A crucial aspect to be considered is that the sensitivity (responsiveness) of the membrane can be tuned by controlling the degree of cross-linking. This is particularly

important because the responsiveness of the material to pH allows for effective cleaning of the membrane, e.g., without the necessity of harsh chemicals. In general, the permeability of polymer materials toward solutes is greatly affected by the degree of cross-linking. Milster *et al.* studied the effects of cross-linking ratio on the solute permeability as well as diffusion via coarse-grained computer simulations.[248] According to their study, permeability can be tuned over an extended range compared to the permeability of bulk polymer materials.

C. Liquid-gated membranes

The capillary-stabilized liquid inside the micro/nanopores of a liquid-infused membrane gives rise to unique dynamic and interfacial properties.[167] As schematically shown in Fig. 7, the dynamic gating concept caused the pore to open for (applied) pressure higher than a threshold value, namely, capillary pressure [see Eq. (4)]. For pressures lower than this threshold, the pore will close since this is thermodynamically favorable.[191] The pressure threshold is a unique property of the membrane determined by many factors, e.g., the geometry of the pores, surface interactions, and the surface tension according to the Young–Laplace equation. Young and Laplace in 1805[249] showed that the pressure difference, ΔP, across a curved fluid interface is directly proportional to its curvature κ, with the interfacial tension γ being the proportionality constant,

$$\Delta P = \gamma \kappa. \tag{1}$$

The curvature of a sphere or semi-sphere [similar to the liquid interface in liquid-filled pores (see the dashed curvature in Fig. 7, middle right)] is defined as $\kappa = \frac{2}{R}$.[250] This is defined based on the universal definition of the curvature $\kappa = 1/R_1 + 1/R_2$, where R_1 and R_2 are the two orthogonal radii of the osculating circles. For a spherically shaped interface, R_1 and R_2 are equal. Thus, the Young–Laplace equation, which is also known as the capillary pressure equation, takes the general form of

$$\Delta P = \frac{2\gamma}{R}. \tag{2}$$

When the liquid is in contact with a solid surface (liquid–solid interface), the wetting state (determined by the surface interactions) of the solid by the liquid must also be considered. The wetting state (wettability) of the solid surface is usually measured/characterized by Young's contact angle θ of a liquid droplet on top of this surface.[111] θ is the angle formed by a liquid at the three-phase boundary where the liquid, gas, and the solid surface intersect.[156] Young's equation is given by

$$\cos\theta = \frac{\gamma_{SA} - \gamma_{SL}}{\gamma_{LA}}, \tag{3}$$

where γ_{SA}, γ_{SL}, and γ_{LA} are the solid–air, solid–liquid, and liquid–air interfacial tension, respectively (see Fig. 2, top left). When $\theta = 180°$, no spreading takes place. This means that the droplet forms a complete sphere located on the surface in the case of low Bond/Eötvös number $Bo = \Delta\rho g L^2/\gamma$, where $\Delta\rho$ is the density difference between the two phases (in units of kg/m^3), g is the gravitational acceleration (in units of m/s^2), and L is the characteristic length [radii of curvature of the drop (in units of m)]. When $\theta = 0°$, full spreading on the

surface takes place. This means that the liquid droplet completely wets the solid surface.[156] Incorporating the wetting behavior of the solid surface in the Young–Laplace equation [Eq. (2)] yields

$$\Delta P = \frac{2\gamma \cos \theta}{R}, \qquad (4)$$

where γ is the interfacial tension between fluids in contact with each other and R is the radius of curvature of the interface. This equation is known as Young–Laplace/capillary pressure, which is used to determine the threshold pressure value of liquid-infused gates.

In the case of liquid-infused membranes, the infusion liquid completely wets and strongly adheres to the porous solid material of the membrane, leading to a contact angle of $0°$ between the infusion liquid and membrane material. As explained in Sec. III, this is an important design criteria which once satisfied, the infusion liquid can completely seal the membrane pores and form a continuous liquid layer along the membrane surface. The design and choice of the infusion liquid to construct a stable liquid gating system highly depends on the application, type of the solid substrate, and the testing liquid.[127,251] In all cases, the infusion liquid should be chemically compatible with the solid substrate and immiscible with the testing/transport liquid. Preston *et al.* developed a model that can accurately predict possible combinations between the infusion liquid, the solid, and the testing liquid in liquid-infused surfaces.[251] Obtaining stable liquid-filled pores discussed here is based on the inherent assumption that no phase change (from liquid to gas) occurs in the infusion liquid. In the case of a volatile infusion liquid, unwanted liquid evaporation or drying can occur, leading to a loss of gating performance. Besides the evident immiscibility requirement (between the infusion and the permeating phases), very low solubility can still cause removal of the infusion liquid over time, which significantly disrupts the gating performance.

In the case of liquid gating systems, the infusion liquid is also designed based on the desired functionality. For example, Sheng *et al.* used magneto-rheological fluid (microscale magnetic colloidal particles stabilized in nonmagnetic fluid using a surfactant) to obtain liquid gating in 3D foam networks.[252] To obtain capillary stabilization of the colloidal suspension in the foam structure, the diameter of the magnetic particles was chosen to be similar to the size of confined spaces in the foam. Wang *et al.* designed host–guest functional gating liquids used to impregnate hydrophilic nylon membranes.[253] Hosts, such as macrocyclic molecules, and guests, such as surfactants, are used. The choice of appropriate host–guest couples is crucial to achieve the required interactions and recognition for applications concerning chemical detection. The affinity between the gating liquid and the membrane substrate can also be modulated on demand to achieve fully closed liquid gates or liquid-lined pathways. Chen *et al.* used glycerol/water mixture as the infusion liquid in thermo-responsive porous membranes obtained by grafting poly(N-isopropylacrylamide) (PNIPAAm) on commercial nylon membranes.[254] At temperatures below the lower critical solution temperature (LCST) of PNIPAAm, there is high affinity between the gating liquid and the thermo-responsive membrane, guaranteeing a capillary-stabilized liquid gate. As the temperature increases (above LCST), the surface wetting behavior changes, leading to poor wetting of the membrane by the gating liquid. The substrate is thus

modified to possess responsive behavior to both temperature and wettability changes. Regardless of the temperature value, with a mild flow of air, an open liquid-lined pathway is obtained from the fully sealed pores. Yu *et al.* used a series of infusion liquids, such as perfluoropolyether, silicone oil, and dichloromethane to design liquid gating emulsification systems.[255] With dodecane as the dispersed and aqueous-based solutions as the continuous phases in the emulsion, dichloromethane and silicon oils showed unstable systems (experimentally and theoretically) due to miscibility with the other phases. To achieve such stable systems, the gating liquid should (i) be completely immiscible with the continuous and dispersed phases of the emulsion and (ii) have higher density compared to that of both phases. Gating liquids with lower densities can get mixed with the other phases upon emulsification, leading to unstable systems and complete removal of the gating liquid from the porous substrate. These principles are crucial to prevent the replacement of the gating liquid by the other phases, ensuring stable emulsification. Zhang *et al.* designed photo-responsive gating liquids by dissolving azobenzene-based surfactants in N,N-dimethylacetamide (DMAC) to fabricate photo-responsive gating membranes.[204] The surface tension of the gating liquid changes upon reversible photoisomerization of the surfactant molecules under different types of light irradiation. This leads to a reversible change in the critical pressure of the gas, resulting in a reversible switch between open and close states. Detailed discussions on the selection of the gating liquid and its governing parameters, e.g., surface tension, viscosity, volatility, the interaction with the porous substrate, and preparation procedure are given in reviews by Yu *et al.*[256] and Sheng *et al.*[257] More detailed explanations about the specific applications of the above-mentioned liquid gating systems are given in Sec. V.

For transport of any fluid, e.g., gases or liquids through the liquid-infused pores, the interface of the infusion liquid must be deformed such that the other fluid can enter the membrane pores. Depending on the physical characteristics of the fluid (e.g., the interfacial tension with the infusion liquid), the corresponding threshold/critical pressure (Young–Laplace pressure) may differ. When the pressure of the system is higher than the critical pressure, the infusion liquid will be partly removed and will form a liquid-lined pathway for passage of the transport fluid while staying attached to the pore wall (see Fig. 7, bottom right). This is because the affinity of the infusion liquid for the membrane is higher than the affinity for the transport fluid (as described earlier in Sec. II). When the transport fluid is immiscible with the infusion liquid, it will flow through without contacting the solid surface of the membrane. This phenomenon is similar to the capillary fingering regime in immiscible displacement in porous media.[258] Capillary fingering is encountered in drainage processes (in oil recovery from reservoirs) where the wetting/defending fluid is displaced by the non-wetting/invading fluid, leaving a layer of wetting liquid attached to the reservoir pore walls. The displacement mechanism in liquid-infused membranes and its similarity to capillary fingering are studied in detail by Bazyar *et al.*[186] Compared to the pristine membrane, without any infusion liquid, this can further prevent fouling since there is no (direct) contact of the transport fluid with the solid surface of the membrane.[157,158,167] Once pressurizing is stopped, the liquid-lined pores inside the membrane return to their original closed state (liquid reinfusion) in the case that sufficient infusion liquid is present.[167,185] Liquid reinfusion strongly depends on the design

of the gating liquid, flow rate of the transport fluid, pore size, and morphology of the porous membrane. This has been demonstrated for gases displacing liquid-filled porous membranes.[185] The "on/off" function of the liquid-infused pores in response to the system pressure makes them responsive gates that can be used for multiphase transport and efficient sorting of immiscible liquids. This will be discussed further in Sec. V. The pressure-responsive opening/closing function of the liquid-infused pores provides a unified platform for facilitating tunable and selective antifouling multiphase transport.[167]

V. APPLICATIONS OF GATING MEMBRANES

As explained earlier in Sec. IV, the permeability and selectivity of smart gating membranes can be controlled in stimuli-responsive (positively and negatively responsive) gates owing to the tunability of pore size and surface properties. In liquid-gated membranes, the dynamic movement of the infusion liquid inside the pores (upon change in the system pressure) is a means to achieve the "on/off" functionality of the pores in a reversible manner. This leads to an adaptive gating behavior to obtain selectivity for the gas–liquid mixtures.[167,191]

For various applications spanning from the detection of ions in water and water purification, to the controlled release, gating membranes can be a powerful tool due to the self-regulation of permeability.[246,259,260] The permeability of membranes with negatively responsive gating behavior based on Pb^{2+} decreases in the presence of minute quantity of Pb^{2+} ions in the solution.[259] The combination of biologically active and pH-responsive (gating) membranes grants the possibility of degrading toxic organics in a membrane-based water purification system. For instance, doped pH-responsive gates (based on PAAc hydrogel) with iron species are a means to achieve toxic organic degradation via decomposition of hydrogen peroxide into free radical oxidants.[260] The toxic organics are degraded into alkali ions, leading to an increase in the pH, which is required for pore closure. The closing state of the pore reduces the permeating flux of toxic organics, providing a longer period for the efficient degradation of these organic materials. For controlled release applications, the diffusion of active molecules (led by the concentration gradient) and the corresponding mass transfer should be regulated. Gating pores with the self-adjustment of permeability based on the diffusion of specific molecules ("diffusional permeability") are efficient platforms for this unique application.[108] As an example, the negatively pH-responsive gating membranes can act as operational valves in an enclosed system for the controlled release of the substances of choice. On the other hand, positively pH-responsive gating membranes can function as a pump to drain the substances in the open state of pores.[246] The release rate is superior compared to that obtained from concentration-driven diffusion.

Both pH- and temperature-responsive membranes with self-adjusting pore size provide an efficient platform for the separation of compounds of varied sizes.[243,247] Depending on the pH of the environment, the pH-responsive membranes selectively reject molecules above a certain molecular weight (such as dextran) in a mixture containing molecules with various molecular weights.[247] In a positively thermo-responsive gating membrane, small molecules (e.g., NaCl) can be permeated at low values of temperature when the pores get smaller, while the permeation of larger molecules is possible at higher values of temperature and, thus, the open state of the pores.[243] The affinity between the pore material and the substances in the stimuli-responsive gating membranes can be controlled owing to the self-adjustment of surface properties. This is of great importance for purification/concentration of compounds such as chiral molecules and proteins.[215] For instance, thermo-responsive gating membranes, which can switch the surface wetting properties between hydrophobic and hydrophilic states (upon changes in the temperature), are useful for the separation (adsorption) of hydrophobic substances, e.g., bovine serum albumin (BSA).[217] In the hydrophobic state of pores, the BSA get adsorbed, whereas it is desorbed in the hydrophilic state. In a recent review article by Bandehali *et al.*, the overall perspective toward the application of various types of smart gating membranes for water treatment purposes is detailed.[109] The corresponding design schemes, separation mechanisms, and the challenges encountered during fabrication are reviewed.

Self-cleaning functionality can be achieved to reduce membrane fouling while retaining the permeability. Typical polymers that are utilized for the fabrication of membranes possess hydrophobic character. Due to these hydrophobic interactions, the organic substances (foulants) prefer to attach on the membrane surface, leading to fouling.[209] Grafting hydrophilic polymers on membrane surfaces has been shown to reduce foulant adsorption.[261] The main issue with the grafted polymers is that they reduce the intrinsic permeability of the membrane as they can partly block the pores.[262] In smart gating membranes with self-cleaning ability, the shrunk and hydrophobic gates become swollen and hydrophilic upon exposure to the stimulus. The hydrophobic–hydrophilic transition can diminish the interaction between the foulant material and the membrane surface, leading to easy removal of the fouling layer by washing with water.[108] The permeability of the membrane will be preserved by recovering the gates to the shrunken state. In a recent review article by Zhang *et al.*, the basics of membrane fouling are summarized along with the progress and advances in nature-inspired antifouling membranes.[110]

The gating mechanism of liquid-infused pores (reversible switch between the "on/off" states) is a powerful tool to manifest selective separation of gases or liquids from a mixture. As explained in Sec. IV, for the permeating phase (gas or liquid) to enter the liquid-infused pore at the corresponding critical pressure [Young–Laplace equation (4)], the gas/liquid or liquid/liquid interface must be deformed. Liquid-gated membranes have a great potential in controllable gas transport applications, in which the permeation of different gases is possible via deformation of the gating liquid meniscus at pressure values above the critical pressure.[167,185,263–266] In applications concerning separation of gases from liquids, two critical (threshold) pressure values (namely, $P_{critical,g}$ and $P_{critical,l}$) exist to selectively permeate the gas or the liquid phase. For example, gas (air)-free water can be obtained by setting the system pressure between the two critical pressure values, i.e., higher than $P_{critical,g}$ and lower than $P_{critical,l}$, to permeate only the gas phase.[167] Self-driven systems for gas/liquid transport regulations have been designed using liquid-gated magnetoelastic porous membranes with reversible deformations.[267] The system stability, non-fouling performance, and tunability were investigated both experimentally and theoretically. On demand, separation of gas–liquid mixtures has been achieved via photothermally induced liquid

gating systems.[268] Light illumination, and photothermal energy thereof, causes a change in the surface/interfacial tension of the gating liquid, leading to the redistribution of the liquid by interfacial tension gradients (i.e., Marangoni flow). Based on the same concept, more complex fluid dispersions can be simply separated. Each component of the multiphase dispersion possesses a distinct critical pressure based on the interfacial tension value with the infusion liquid. This, for instance, can be beneficial for oily wastewater treatment applications. The discharged oily wastewater streams (from domestic or industrial plants) containing oil/water mixtures pose a serious danger for both the environment and human health.[213,269] Membrane-based separation technology provides an efficient tool for oily wastewater treatment, which has been the focus of a significant number of studies.[270–274] Unlike conventional membrane-based oil/water separation techniques (in which the continuous phase is being permeated), in liquid-gated membranes, the minor phase, i.e., oil, can be selectively permeated while retaining the continuous water phase.[187,275] This is economically beneficial, specially at low oil concentrations. In a recent study by Song and Rutledge, the mechanism of oil transport through liquid-infused membranes has been examined.[275] A linear relationship was found between the permeating oil flux and the oil concentration in the feed. Song and Rutledge[275] provide guidelines for the design of composite liquid-infused membranes and the choice of operating parameters. Wetting properties of liquid-gated membranes can be regulated by infusing liquids with different surface energies. The interaction between the polarity of various infusion liquids and the membrane material provides the possibility of developing adaptable separation.[276] In this case, no external stimulation or covalent modification is necessary. In addition to the above-mentioned applications, the anti-biofouling properties of liquid-gated membranes have been demonstrated. After fouling with protein and/or bacteria, the permeated flux through these membranes can be recovered without the need for harsh cleaning agents or antibiotics.[277] Among various types of membrane fouling, biofouling (attachment and accumulation of living foulant materials on the membrane surface or on the pore wall) contributes to ~45%.[278,279] The anti-biofouling performance is attributed to the presence of liquid-lined pores, which inhibit the formation of a permanent contact between the foulant material and the membrane pore wall. The liquid-infused pores are capable of mitigating biofouling in long-term cross flow filtration modes. A substantial decrease in the growth rate of bacteria has been observed.[158] Experiments at industrially relevant transmembrane pressures have demonstrated no or minor loss of infusion liquid and maintaining antifouling properties.[280] In a recent application, liquid gating membranes were used in a highly efficient emulsification process.[255] The formed liquid–liquid interface between the gating liquid, disperse and continuous phases at the pore scale provides enough shear stress to break the dispersed liquid phase into droplets with narrow size distribution. The slippery and drag-reducing interface decreases the fouling as well as resistance, leading to an energy-efficient emulsification process.

Examples of new industrial application areas of liquid-gated membranes include visual chemical detection[281] and smart piston and valve applications.[265] The pressure-driven movement of the liquid [see Fig. 6 (bottom right)] can function as a piston.[265] Smart valve functionality can be achieved by incorporating loosely cross-linked polymers (such as pneumatic elastomers) into the

liquid-gated membrane systems. The dynamic gas/liquid interface in a liquid gating system can also be used as a chemical detection mechanism via dipole-induced interfacial molecular reconfiguration.[281] The dipole forces can rearrange the molecules present on the interface, leading to a change in the gating behavior. This can be used as a visual sign for chemical detection purposes. Since no electrical energy is required, this detection method is considered as a "green" alternative. Visual chemical detection using liquid gating mechanism has been used as an *in situ* sensing platform for visual quantification of target molecules.[253] The system has been tested experimentally and theoretically, showing specificity and scalability for applications spanning from food analysis to drug testing. Liquid gating systems have found applications in tuning the dynamics of confined stimuli-responsive colloidal particles.[252] The mechanical properties of the colloidal suspension and transport properties of the solvent can be tuned by the external field, such as magnetic field, depending on the type of stimuli-responsive particles. Smart gas valves have been designed using dynamic liquid gating within light-responsive solid porous substrates. The inert gating liquid inhibits the solid substrate from corroding, providing a precisely controlled switch under constant pressure.[282] Recently, CO_2 gas valves have been introduced using chemically responsive liquid gating membranes.[283] The acidification of liquid due to the dissolution of CO_2 changes the transmembrane critical pressure, leading to self-adaptive regulations with different CO_2 concentrations. In a recent work, liquid gating was used to design thermal adaptive systems producing smart breathing to regulate indoor temperature with lower energy consumption.[254] The "sandwich" structure of liquid-filled thermo-responsive porous membranes provides different opening profiles for different temperature ranges around a desired set point. The thermal adaptive system has been tested as greenhouse patches, showing enhanced energy-saving performance based on experimental and simulation studies. Liquid-gated systems have found promising applications in the biomedical field as well. For example, liquid gating membrane-based catheters have been designed that can significantly impair blood clot formation (thrombosis) and promote controlled drug release.[284]

VI. SUMMARY

Nature has been a perennial source of inspiration for the design and creation of new materials. With the advances made in the field of science and manufacturing technologies in the past few decades, various nature-inspired materials, structures, designs, and even algorithms have been developed. Many phenomena in nature deal with wettability. Examples of surfaces with remarkable wettability in nature include the lotus leaf, pitcher plant, rice leaf, and cicada wings. Thus, significant efforts have been devoted to studying surface wettability and to uncovering the underlying mechanisms. In this Review, nature-inspired surfaces with special wettability, namely, superhydrophobic surfaces, and slippery liquid-infused surfaces (SLIPS) were introduced. With specific focus on SLIPS, the working mechanism, fabrication principles/strategies, properties, design criteria, and application fields were explained in detail. We further narrowed down the concept of liquid-infused surfaces to the field of membrane technology. Slippery liquid-infused membranes (SLIMs) were introduced and the corresponding applications, design criteria, and fabrication methods were detailed. The infusion liquid, which is stabilized in the membrane pores via

capillary forces, leads to the formation of a reversible gate that opens/closes in response to a stimulus, i.e., pressure (liquid gating membranes). The gating of the membrane mimics the functionality of biological systems in nature, such as smell perception in the human body or an electric eel. The ion permeation through biological cell membranes is regulated via gating ion channels with open/close functionality under the presence/change of the corresponding environmental stimuli. With the special capability of gating and the slippery nature, SLIMs belong to the category of smart/stimuli-responsive membranes, which are inspired by nature in terms of both their surface wettability and their gating functionality. In this Review, smart gating membrane systems were introduced and their important features, i.e., self-adjustable permeability and selectivity, were explained. In this Review, smart gating membrane systems were introduced and general design criteria and fabrication schemes were discussed. Important features of these membranes, i.e., self-adjustable permeability and selectivity were further explained. As the most common types of stimuli, fabrication and applications of temperature- and pH-responsive gating membranes were elaborated. Liquid-gated membranes and their corresponding working principles (gating) and requirements were discussed in detail. Finally, application fields of various types of gating membranes (ion-responsive, pH-responsive, temperature-responsive, and liquid-infused) were reviewed.

VII. CHALLENGES AND PERSPECTIVES

Despite the significant developments that have taken place during the last decades in the area of nature-inspired gating membranes as well as slippery liquid-infused surfaces, there still exist challenges that need to be addressed:

(1) *Durability*: The progressive loss of liquid lubricant in SLIMs under industrially relevant shear conditions influences their service life significantly. The gating functionality of most gating membranes may decrease under repetitive responses, leading to irreversible behavior under realistic test conditions. The use of an appropriate solid lubricant can address this issue, but it requires an additional stimulus, i.e., temperature to activate the gating functionality. Establishing a strong interaction between the lubricant and solid surface (binding), not only based on chemical compatibility, can be an alternative approach to improve the stability of liquid gates.

(2) *Mechanical robustness*: Gating behavior relies on the presence of functional moieties on the surface of membrane or the pore wall material. The instability or weak mechanical properties of chain-like structures, liquid, hydrogel network, or microspheres can disturb the gating functionality upon application of transmembrane pressure. In a recent study by Ding *et al.*,[195] this issue has been addressed via application of wood-based membranes. Yet, there are various other types of materials that have to be investigated.

(3) *Scalability*: Further adaption of smart gating membranes at the industrial scale requires the availability of easy, cheap, and straightforward fabrication methods with long-term stability. The current fabrication methods do not meet these criteria, making the scalable fabrication of these membranes a challenging task. Bioinspired design strategies can solve this issue, but they require further development of novel functional materials.

(4) *Performance during long-term operation*: One of the key properties of nature-inspired membranes is anti-(bio)fouling. However, this property has been investigated in lab-scale experiments in short-term operation periods. There is a great need for studying the anti-(bio)fouling performance of gating membranes in long-term operations, mimicking the conditions of industrial wastewater treatment. Another important feature is the volatility and miscibility of the infusion liquid. The long-term stability of the infusion liquid under extreme conditions on the gating performance should be investigated.

(5) *Practical applications*: The state-of-the-art in gating membranes is primarily focused on applications involving liquid species. However, applications in which gas/liquid, gas/solid, and solid/liquid systems are involved (e.g., separations, wastewater treatment, air purification) could greatly benefit from the incorporation of membranes with gating mechanisms. Therefore, more experimental efforts should be focused toward this area as well as for extending the commonly studied temperature- and pH-responsive gating membranes, for which reliable measurement data still remain scarce.

(6) *Novel materials and fabrication strategies*: The direct approach for fabricating gating membranes using functional materials is preferred as it does not need further modifications. Although it provides a great potential for easy scale-up as well as efficient industrial manufacturing, its application has been restricted due to the limited options available for functional materials. To address this issue, two approaches can be considered: *(i)* developing entirely novel stimuli-responsive materials (for instance, based on dynamic chemistry), and *(ii)* developing innovative geometric designs to create smart and multi-functional gating systems. The latter can be achieved by combining material and design concepts from other disciplines, e.g., bionic, robotics, and meta-materials.

(7) *Advanced fabrication technologies*: The current fabrication procedures of smart gating membranes are complicated, expensive, and energy-intensive. There is an urgent need for the development of advanced and more user-friendly fabrication methods based on, for instance, 3D and/or 4D printing. Fully 3D printed membranes with micro/nanopore sizes are still in their infancy due to limitations in the current state-of-the-art methods, such as printing resolution and limited material types. Further development of 3D printing technology is required to directly print small pores with functional materials.

(8) *Better understanding of mechanisms in biological systems*: There still exist several natural processes and scenarios that have not been explored. To effectively design smart gating membranes for various applications, there is a significant need for exploring new biological processes and fully understanding the underlying principles. Modeling and simulations can be a powerful tool to achieve this goal.

(9) *Exploring applications in other fields*: Smart gating membranes are still at an early stage of development. To

further expand their potential applicability, novel application areas, such as sensing, detection, and valve-based regulation, should be studied in depth.

(10) *Fully sustainable gating systems*: The progressive loss and leakage of functional species in the gating membrane (e.g., fluorinated infusion lubricant in liquid-gated membranes) is a point of concern from an environmental point of view. There is an urgent demand for promoting biolubricants as well as waste-derived/recycled polymers.

ACKNOWLEDGMENTS

AUTHOR DECLARATIONS
Conflict of Interest

The authors have no conflicts to disclose.

Author Contributions

Hanieh Bazyar: Conceptualization (equal); Formal analysis (equal); Methodology (equal); Writing – original draft (equal); Writing – review & editing (equal). **Othonas A. Moultos**: Conceptualization (equal); Writing – review & editing (equal). **Rob G. H. Lammertink**: Conceptualization (equal); Funding acquisition (equal); Supervision (equal); Writing – review & editing (equal).

DATA AVAILABILITY

The data that support the findings of this study are available from the corresponding author upon reasonable request.

REFERENCES

[1]C. Wan, Y. Jiao, D. Liang, Y. Wu, and J. Li, "A geologic architecture system-inspired micro-/nano-heterostructure design for high-performance energy storage," Adv. Energy Mater. **8**, 1802388 (2018).

[2]A. S. Perera and M. O. Coppens, "Re-designing materials for biomedical applications: From biomimicry to nature-inspired chemical engineering," Philos. Trans. R. Soc., A **377**, 20180268 (2019).

[3]P. Fratzl, "Biomimetic materials research: What can we really learn from nature's structural materials?," J. R. Soc., Interface **4**, 637–642 (2007).

[4]N. K. Katiyar, G. Goel, S. Hawi, and S. Goel, "Nature-inspired materials: Emerging trends and prospects," NPG Asia Mater. **13**, 56 (2021).

[5]J. Peng and Q. Cheng, "High-performance nanocomposites inspired by nature," Adv. Mater. **29**, 1702959 (2017).

[6]U. G. K. Wegst, H. Bai, E. Saiz, A. P. Tomsia, and R. O. Ritchie, "Bioinspired structural materials," Nat. Mater. **14**, 23–36 (2015).

[7]H.-B. Yao, H.-Y. Fang, X.-H. Wang, and S.-H. Yu, "Hierarchical assembly of micro-/nano-building blocks: Bio-inspired rigid structural functional materials," Chem. Soc. Rev. **40**, 3764–3785 (2011).

[8]W. Zhang and W. Zheng, "Exsolution-mimic heterogeneous surfaces: Towards unlimited catalyst design," ChemCatChem **7**, 48–50 (2015).

[9]T. Sun, L. Feng, X. Gao, and L. Jiang, "Bioinspired surfaces with special wettability," Acc. Chem. Res. **38**, 644–652 (2005).

[10]T. Nishino, M. Meguro, K. Nakamae, M. Matsushita, and Y. Ueda, "The lowest surface free energy based on –CF$_3$ alignment," Langmuir **15**, 4321–4323 (1999).

[11]L. Feng, S. Li, Y. Li, H. Li, L. Zhang, J. Zhai, Y. Song, B. Liu, L. Jiang, and D. Zhu, "Super-hydrophobic surfaces: From natural to artificial," Adv. Mater. **14**, 1857–1860 (2002).

[12]W. Barthlott and C. Neinhuis, "Purity of the sacred lotus, or escape from contamination in biological surfaces," Planta **202**, 1–8 (1997).

[13]C. Neinhuis and W. Barthlott, "Characterization and distribution of water-repellent, self-cleaning plant surfaces," Ann. Bot. **79**, 667–677 (1997).

[14]C. Luo, H. Zheng, L. Wang, H. Fang, J. Hu, C. Fan, Y. Cao, and J. Wang, "Direct three-dimensional imaging of the buried interfaces between water and superhydrophobic surfaces," Angew. Chem., Int. Ed. **49**, 9145–9148 (2010).

[15]Y. Zheng, X. Gao, and L. Jiang, "Directional adhesion of superhydrophobic butterfly wings," Soft Matter **3**, 178–182 (2007).

[16]X. Gao, X. Yan, X. Yao, L. Xu, K. Zhang, J. Zhang, B. Yang, and L. Jiang, "The dry-style antifogging properties of mosquito compound eyes and artificial analogues prepared by soft lithography," Adv. Mater. **19**, 2213–2217 (2007).

[17]G. Zhang, J. Zhang, G. Xie, Z. Liu, and H. Shao, "Cicada wings: A stamp from nature for nanoimprint lithography," Small **2**, 1440–1443 (2006).

[18]L. Feng, Y. Zhang, J. Xi, Y. Zhu, N. Wang, F. Xia, and L. Jiang, "Petal effect: A superhydrophobic state with high adhesive force," Langmuir **24**, 4114–4119 (2008).

[19]W. R. Hansen and K. Autumn, "Evidence for self-cleaning in gecko setae," Proc. Natl. Acad. Sci. U. S. A. **102**, 385–389 (2005).

[20]K. Liu, J. Du, J. Wu, and L. Jiang, "Superhydrophobic gecko feet with high adhesive forces towards water and their bio-inspired materials," Nanoscale **4**, 768–772 (2012).

[21]A. R. Parker and C. R. Lawrence, "Water capture by a desert beetle," Nature **414**, 33–34 (2001).

[22]X. Gao and L. Jiang, "Water-repellent legs of water striders," Nature **432**, 36 (2004).

[23]D. Richard and D. Quéré, "Viscous drops rolling on a tilted non-wettable solid," Europhys. Lett. **48**, 286–291 (1999).

[24]D. Richard and D. Quéré, "Bouncing water drops," Europhys. Lett. **50**, 769–775 (2000).

[25]D. Quéré, "Rough ideas on wetting," Physica A **313**, 32–46 (2002).

[26]H. J. Ensikat, P. Ditsche-Kuru, C. Neinhuis, and W. Barthlott, "Superhydrophobicity in perfection: The outstanding properties of the lotus leaf," Beilstein J. Nanotechnol. **2**, 152–161 (2011).

[27]Y. T. Cheng, D. E. Rodak, C. A. Wong, and C. A. Hayden, "Effects of micro- and nano-structures on the self-cleaning behaviour of lotus leaves," Nanotechnology **17**, 1359–1362 (2006).

[28]K. Koch, B. Bhushan, Y. C. Jung, and W. Barthlott, "Fabrication of artificial lotus leaves and significance of hierarchical structure for superhydrophobicity and low adhesion," Soft Matter **5**, 1386–1393 (2009).

[29]M. A. Samaha, H. V. Tafreshi, and M. Gad-el-Hak, "Superhydrophobic surfaces: From the lotus leaf to the submarine," C. R. Mec. **340**, 18–34 (2012).

[30]See https://www.properla.co.uk/lotus-effect/ for "The lotus effect," (Properla UK, 2022) (Last accessed, May 2022).

[31]B. B. from Biology, The lotus effect. Water forms droplets on the tips of the epidermal, 2022.

[32]T. Onda, S. Shibuichi, N. Satoh, and K. Tsujii, "Super-water-repellent fractal surfaces," Langmuir **12**, 2125–2127 (1996).

[33]W. Chen, A. Y. Fadeev, M. C. Hsieh, D. Öner, J. Youngblood, and T. J. McCarthy, "Ultrahydrophobic and ultralyophobic surfaces: Some comments and examples," Langmuir **15**, 3395–3399 (1999).

[34]H. Li, X. Wang, Y. Song, Y. Liu, Q. Li, L. Jiang, and D. Zhu, "Super-'amphiphobic' aligned carbon nanotube films," Angew. Chem., Int. Ed. **40**, 1743–1746 (2001).

[35]H. Y. Erbil, A. L. Demirel, Y. Avcı, and O. Mert, "Transformation of a simple plastic into a superhydrophobic surface," Science **299**, 1377–1380 (2003).

[36]L. Vogelaar, R. G. H. Lammertink, and M. Wessling, "Superhydrophobic surfaces having two-fold adjustable roughness prepared in a single step," Langmuir **22**, 3125–3130 (2006).

[37]S. Nishimoto and B. Bhushan, "Bioinspired self-cleaning surfaces with superhydrophobicity, superoleophobicity, and superhydrophilicity," RSC Adv. **3**, 671–690 (2013).

[38]K. M. Wisdom, J. A. Watson, X. Qu, F. Liu, G. S. Watson, and C.-H. Chen, "Self-cleaning of superhydrophobic surfaces by self-propelled jumping condensate," Proc. Natl. Acad. Sci. U. S. A. **110**, 7992–7997 (2013).

[39]P. Guo, Y. Zheng, M. Wen, C. Song, Y. Lin, and L. Jiang, "Icephobic/anti-icing properties of micro/nanostructured surfaces," Adv. Mater. **24**, 2642–2648 (2012).

[40]S. Bengaluru Subramanyam, V. Kondrashov, J. Rühe, and K. K. Varanasi, "Low ice adhesion on nano-textured superhydrophobic surfaces under supersaturated conditions," ACS Appl. Mater. Interfaces **8**, 12583–12587 (2016).

[41]N. K. Mandsberg and R. Taboryski, "Spatial control of condensation on chemically homogeneous pillar-built surfaces," Langmuir **33**, 5197–5203 (2017).

[42]J. B. Boreyko and C. H. Chen, "Self-propelled dropwise condensate on superhydrophobic surfaces," Phys. Rev. Lett. **103**, 184501 (2009).

[43]J. Ou, B. Perot, and J. P. Rothstein, "Laminar drag reduction in microchannels using ultrahydrophobic surfaces," Phys. Fluids **16**, 4635–4643 (2004).

[44]J. Ou and J. P. Rothstein, "Direct velocity measurements of the flow past drag-reducing ultrahydrophobic surfaces," Phys. Fluids **17**, 103606 (2005).

[45]C. Lee, C. H. Choi, and C. J. Kim, "Structured surfaces for a giant liquid slip," Phys. Rev. Lett. **101**, 064501 (2008).

[46]C. Lee and C.-J. C. Kim, "Maximizing the giant liquid slip on superhydrophobic microstructures by nanostructuring their sidewalls," Langmuir **25**, 12812–12818 (2009).

[47]C. H. Choi and C. J. Kim, "Large slip of aqueous liquid flow over a nanoengineered superhydrophobic surface," Phys. Rev. Lett. **96**, 066001 (2006).

[48]E. Karatay, A. S. Haase, C. W. Visser, C. Sun, D. Lohse, P. A. Tsai, and R. G. H. Lammertink, "Control of slippage with tunable bubble mattresses," Proc. Natl. Acad. Sci. U. S. A. **110**, 8422–8426 (2013).

[49]E. G. Shafrin and W. A. Zisman, "Constitutive relations in the wetting of low energy surfaces and the theory of the retraction method of preparing monolayers," J. Phys. Chem. **64**, 519–524 (1960).

[50]T. P. Nhung Nguyen, P. Brunet, Y. Coffinier, and R. Boukherroub, "Quantitative testing of robustness on superomniphobic surfaces by drop impact," Langmuir **26**, 18369–18373 (2010).

[51]L. Zheng, R. Shafack, B. Walker, and K. Chan, "The impact of high humidity on the ice-phobicity of copper-based superhydrophobic surfaces," Nanomater. Nanotechnol. **7**, 1 (2017).

[52]M. He, H. Li, J. Wang, and Y. Song, "Superhydrophobic surface at low surface temperature," Appl. Phys. Lett. **98**, 093118 (2011).

[53]P. Papadopoulos, L. Mammen, X. Deng, D. Vollmer, and H.-J. Butt, "How superhydrophobicity breaks down," Proc. Natl. Acad. Sci. U. S. A. **110**, 3254–3258 (2013).

[54]R. Di Mundo, F. Bottiglione, M. Notarnicola, F. Palumbo, and G. Pascazio, "Plasma-textured teflon: Repulsion in air of water droplets and drag reduction underwater," Biomimetics **2**(1), 1 (2017).

[55]T. Koishi, K. Yasuoka, S. Fujikawa, T. Ebisuzaki, and X. C. Zeng, "Coexistence and transition between Cassie and Wenzel state on pillared hydrophobic surface," Proc. Natl. Acad. Sci. U. S. A. **106**, 8435–8440 (2009).

[56]T. Deng, K. K. Varanasi, M. Hsu, N. Bhate, C. Keimel, J. Stein, and M. Blohm, "Nonwetting of impinging droplets on textured surfaces," Appl. Phys. Lett. **94**, 133109 (2009).

[57]A. B. D. Cassie and S. Baxter, "Wettability of porous surfaces," Trans. Faraday Soc. **40**, 546–551 (1944).

[58]R. N. Wenzel, "Resistance of solid surfaces to wetting by water," Ind. Eng. Chem. **28**, 988–994 (1936).

[59]M. Sbragaglia, A. M. Peters, C. Pirat, B. M. Borkent, R. G. Lammertink, M. Wessling, and D. Lohse, "Spontaneous breakdown of superhydrophobicity," Phys. Rev. Lett. **99**, 156001 (2007).

[60]Z. Ashrafi, L. Lucia, and W. Krause, "Nature-inspired liquid infused systems for superwettable surface energies," ACS Appl. Mater. Interfaces **11**, 21275–21293 (2019).

[61]Y.-J. Sheng, S. Jiang, and H.-K. Tsao, "Effects of geometrical characteristics of surface roughness on droplet wetting," J. Chem. Phys. **127**, 234704 (2007).

[62]G. Pashos, G. Kokkoris, A. G. Papathanasiou, and A. G. Boudouvis, "Wetting transitions on patterned surfaces with diffuse interaction potentials embedded in a Young-Laplace formulation," J. Chem. Phys. **144**, 034105 (2016).

[63]E. Kierlik, M. L. Rosinberg, Y. Fan, and P. A. Monson, "Prewetting at a liquid mixture–solid interface: A comparison of Monte Carlo simulations with mean field density functional theory," J. Chem. Phys. **101**, 10947–10952 (1994).

[64]M. Schneemilch, N. Quirke, and J. R. Henderson, "Wetting of nanopatterned surfaces: The striped surface," J. Chem. Phys. **118**, 816–829 (2003).

[65]K. Luo, M.-P. Kuittu, C. Tong, S. Majaniemi, and T. Ala-Nissila, "Phase-field modeling of wetting on structured surfaces," J. Chem. Phys. **123**, 194702 (2005).

[66]V. Kumar, S. Sridhar, and J. R. Errington, "Monte Carlo simulation strategies for computing the wetting properties of fluids at geometrically rough surfaces," J. Chem. Phys. **135**, 184702 (2011).

[67]V. Kumar and J. R. Errington, "Understanding wetting of immiscible liquids near a solid surface using molecular simulation," J. Chem. Phys. **139**, 064110 (2013).

[68]A. Malijevský, "Does surface roughness amplify wetting?," J. Chem. Phys. **141**, 184703 (2014).

[69]Y. Zhang and W. Ren, "Numerical study of the effects of surface topography and chemistry on the wetting transition using the string method," J. Chem. Phys. **141**, 244705 (2014).

[70]M. Svoboda, A. Malijevský, and M. Lísal, "Wetting properties of molecularly rough surfaces," J. Chem. Phys. **143**, 104701 (2015).

[71]R. Evans, M. C. Stewart, and N. B. Wilding, "Drying and wetting transitions of a Lennard-Jones fluid: Simulations and density functional theory," J. Chem. Phys. **147**, 044701 (2017).

[72]K. Jain, A. J. Schultz, and J. R. Errington, "Application of the interface potential approach for studying wetting behavior within a molecular dynamics framework," J. Chem. Phys. **150**, 204118 (2019).

[73]W. Guo and J. R. Errington, "Effect of carboxylic acid on the wetting properties of a model water–octane–silica system," Langmuir **35**, 6540–6549 (2019).

[74]K. Jain, K. S. Rane, and J. R. Errington, "Using isothermal-isobaric Monte Carlo simulation to study the wetting behavior of model systems," J. Chem. Phys. **150**, 084110 (2019).

[75]W. Guo and J. R. Errington, "Monte Carlo simulation strategies to compute the interfacial properties of a model octane–water–silica system," J. Phys. Chem. C **122**, 17309–17318 (2018).

[76]V. Kumar and J. R. Errington, "The use of Monte Carlo simulation to obtain the wetting properties of water," Phys. Procedia **53**, 44–49 (2014).

[77]V. Kumar and J. R. Errington, "Application of the interface potential approach to calculate the wetting properties of a water model system," Mol. Simul. **39**, 1143–1152 (2013).

[78]V. Kumar and J. R. Errington, "Impact of small-scale geometric roughness on wetting behavior," Langmuir **29**, 11815–11820 (2013).

[79]V. Kumar and J. R. Errington, "Wetting behavior of water near nonpolar surfaces," J. Phys. Chem. C **117**, 23017–23026 (2013).

[80]K. S. Rane, V. Kumar, and J. R. Errington, "Monte Carlo simulation methods for computing the wetting and drying properties of model systems," J. Chem. Phys. **135**, 234102 (2011).

[81]V. Kumar and J. R. Errington, "Monte Carlo simulation strategies to compute interfacial and bulk properties of binary fluid mixtures," J. Chem. Phys. **138**, 174112 (2013).

[82]A. J. Patel, P. Varilly, and D. Chandler, "Fluctuations of water near extended hydrophobic and hydrophilic surfaces," J. Phys. Chem. B **114**, 1632–1637 (2010).

[83]P. Bratko, S. Perkin, H. Christenson, R.-H. Yoon, and A. Patel, "Wetting dynamics of hydrophobic and structured surfaces: General discussion," Faraday Discuss. **146**, 367–393 (2010).

[84]R. C. Remsing, E. Xi, S. Vembanur, S. Sharma, P. G. Debenedetti, S. Garde, and A. J. Patel, "Pathways to dewetting in hydrophobic confinement," Proc. Natl. Acad. Sci. U. S. A. 112, 8181–8186 (2015).

[85]S. Prakash, E. Xi, and A. J. Patel, "Spontaneous recovery of superhydrophobicity on nanotextured surfaces," Proc. Natl. Acad. Sci. U. S. A. 113, 5508–5513 (2016).

[86]H. Jiang, S. Fialoke, Z. Vicars, and A. J. Patel, "Characterizing surface wetting and interfacial properties using enhanced sampling (SWIPES)," Soft Matter 15, 860–869 (2019).

[87]H. Jiang and A. J. Patel, "Recent advances in estimating contact angles using molecular simulations and enhanced sampling methods," Curr. Opin. Chem. Eng. 23, 130–137 (2019).

[88]E. S. Savoy and F. A. Escobedo, "Simulation study of free-energy barriers in the wetting transition of an oily fluid on a rough surface with reentrant geometry," Langmuir 28, 16080–16090 (2012).

[89]S. Khan and J. K. Singh, "Wetting transition of nanodroplets of water on textured surfaces: A molecular dynamics study," Mol. Simul. 40, 458–468 (2014).

[90]H. Yaghoubi and M. Foroutan, "Molecular investigation of the wettability of rough surfaces using molecular dynamics simulation," Phys. Chem. Chem. Phys. 20, 22308–22319 (2018).

[91]E. E. Santiso, C. Herdes, and E. A. Müller, "On the calculation of solid-fluid contact angles from molecular dynamics," Entropy 15, 3734–3745 (2013).

[92]S. Ravipati, B. Aymard, S. Kalliadasis, and A. Galindo, "On the equilibrium contact angle of sessile liquid drops from molecular dynamics simulations," J. Chem. Phys. 148, 164704 (2018).

[93]C. M. Tenney and R. T. Cygan, "Molecular simulation of carbon dioxide, brine, and clay mineral interactions and determination of contact angles," Environ. Sci. Technol. 48, 2035–2042 (2014).

[94]J. Škvára, J. Škvor, and I. Nezbeda, "Evaluation of the contact angle from molecular simulations," Mol. Simul. 44, 190–199 (2018).

[95]B. Shi and V. K. Dhir, "Molecular dynamics simulation of the contact angle of liquids on solid surfaces," J. Chem. Phys. 130, 034705 (2009).

[96]S. K. Sethi, S. Kadian, and G. Manik, "A review of recent progress in molecular dynamics and coarse-grain simulations assisted understanding of wettability," Arch. Comput. Methods Eng. 29, 3059–3085 (2022).

[97]J. De Coninck and T. D. Blake, "Wetting and molecular dynamics simulations of simple liquids," Annu. Rev. Mater. Res. 38, 1–22 (2008).

[98]H. S. Salehi, O. A. Moultos, and T. J. H. Vlugt, "Interfacial properties of hydrophobic deep eutectic solvents with water," J. Phys. Chem. B 125, 12303–12314 (2021).

[99]K. D. Papavasileiou, O. A. Moultos, and I. G. Economou, "Predictions of water/oil interfacial tension at elevated temperatures and pressures: A molecular dynamics simulation study with biomolecular force fields," Fluid Phase Equilib. 476, 30–38 (2018), part of Special Issue: The Ninth Industrial Fluid Properties Simulation Challenge.

[100]G. A. Orozco, O. A. Moultos, H. Jiang, I. G. Economou, and A. Z. Panagiotopoulos, "Molecular simulation of thermodynamic and transport properties for the H_2O+NaCl system," J. Chem. Phys. 141, 234507 (2014).

[101]H. S. Salehi, H. M. Polat, F. de Meyer, C. Houriez, C. Coquelet, T. J. H. Vlugt, and O. A. Moultos, "Vapor pressures and vapor phase compositions of choline chloride urea and choline chloride ethylene glycol deep eutectic solvents from molecular simulation," J. Chem. Phys. 155, 114504 (2021).

[102]M. Liu, S. Wang, and L. Jiang, "Nature-inspired superwettability systems," Nat. Rev. Mater. 2, 17036 (2017).

[103]A. Grinthal and J. Aizenberg, "Mobile interfaces: Liquids as a perfect structural material for multifunctional, antifouling surfaces," Chem. Mater. 26, 698–708 (2014).

[104]C. Wang and Z. Guo, "A comparison between superhydrophobic surfaces (SHS) and slippery liquid-infused porous surfaces (SLIPS) in application," Nanoscale 12, 22398–22424 (2020).

[105]X. Zeng, Z. Guo, and W. Liu, "Recent advances in slippery liquid-infused surfaces with unique properties inspired by nature," Bio-Des. Manuf. 4, 506–525 (2021).

[106]M. A. Samaha and M. Gad-el-Hak, "Slippery surfaces: A decade of progress," Phys. Fluids 33, 071301 (2021).

[107]T. J. Brodribb, F. Sussmilch, and S. A. M. McAdam, "From reproduction to production, stomata are the master regulators," Plant J. 101, 756–767 (2020).

[108]Z. Liu, W. Wang, R. Xie, X.-J. Ju, and L.-Y. Chu, "Stimuli-responsive smart gating membranes," Chem. Soc. Rev. 45, 460–475 (2016).

[109]S. Bandehali, F. Parvizian, S. M. Hosseini, T. Matsuura, E. Drioli, J. Shen, A. Moghadassi, and A. S. Adeleye, "Planning of smart gating membranes for water treatment," Chemosphere 283, 131207 (2021).

[110]X. Zhang, J. Ma, J. Zheng, R. Dai, X. Wang, and Z. Wang, "Recent advances in nature-inspired antifouling membranes for water purification," Chem. Eng. J. 432, 134425 (2022).

[111]T. Young, "An essay on the cohesion of fluids," Philos. Trans. R. Soc. London 95, 65–87 (1805).

[112]U. Bauer and W. Federle, "The insect-trapping rim of Nepenthes pitchers: Surface structure and function," Plant Signaling Behav. 4, 1019–1023 (2009).

[113]J. A. Moran, L. K. Gray, C. Clarke, and L. Chin, "Capture mechanism in Palaeotropical pitcher plants (Nepenthaceae) is constrained by climate," Ann. Bot. 112, 1279–1291 (2013).

[114]H. F. Bohn and W. Federle, "Insect aquaplaning: Nepenthes pitcher plants capture prey with the peristome, a fully wettable water-lubricated anisotropic surface," Proc. Natl. Acad. Sci. U. S. A. 101, 14138–14143 (2004).

[115]M. Riedel, A. Eichner, and R. Jetter, "Slippery surfaces of carnivorous plants: Composition of epicuticular wax crystals in Nepenthes alata Blanco pitchers," Planta 218, 87–97 (2003).

[116]See https://books.google.nl/books?id=qM1DAAAAIAAJ for New Scientist (New Science Publications, 1962), Vol. 13, 268–281.

[117]L. Gaume, P. Perret, E. Gorb, S. Gorb, J.-J. Labat, and N. Rowe, "How do plant waxes cause flies to slide? Experimental tests of wax-based trapping mechanisms in three pitfall carnivorous plants," Arthropod Struct. Dev. 33, 103–111 (2004), part of Special Issue: Attachment Systems of Arthropods.

[118]E. V. Gorb and S. N. Gorb, "Physicochemical properties of functional surfaces in pitchers of the carnivorous plant Nepenthes alata Blanco (Nepenthaceae)," Plant Biol. 8, 841–848 (2006).

[119]L. Wang, Q. Zhou, Y. Zheng, and S. Xu, "Composite structure and properties of the pitcher surface of the carnivorous plant Nepenthes and its influence on the insect attachment system," Prog. Nat. Sci. 19, 1657–1664 (2009).

[120]I. Scholz, M. Bückins, L. Dolge, T. Erlinghagen, A. Weth, F. Hischen, J. Mayer, S. Hoffmann, M. Riederer, M. Riedel, and W. Baumgartner, "Slippery surfaces of pitcher plants: Nepenthes wax crystals minimize insect attachment via microscopic surface roughness," J. Exp. Biol. 213, 1115–1125 (2010).

[121]E. V. Gorb and S. N. Gorb, "Functional surfaces in the pitcher of the carnivorous plant Nepenthes alata: A cryo-sem approach," in Functional Surfaces in Biology: Adhesion Related Phenomena, edited by S. N. Gorb (Springer Netherlands, Dordrecht, 2009), Vol. 2, pp. 205–238.

[122]L. Gaume and Y. Forterre, "A viscoelastic deadly fluid in carnivorous pitcher plants," PLoS One 2, e1185 (2007).

[123]V. Bonhomme, H. Pelloux-Prayer, E. Jousselin, Y. Forterre, J. J. Labat, and L. Gaume, "Slippery or sticky? Functional diversity in the trapping strategy of Nepenthes carnivorous plants," New Phytol. 191, 545–554 (2011).

[124]See https://www.dmbotanicalgarden.com/event/carnivorous-plant-terrariums/ for "Slippery surface inspired by pitcher plant," (Physics World, 2019) (Last accessed, May 2022).

[125]T.-S. Wong, S. H. Kang, S. K. Y. Tang, E. J. Smythe, B. D. Hatton, A. Grinthal, and J. Aizenberg, "Bioinspired self-repairing slippery surfaces with pressure-stable omniphobicity," Nature 477, 443–447 (2011).

[126]P. Wang, D. Zhang, and Z. Lu, "Slippery liquid-infused porous surface bio-inspired by pitcher plant for marine anti-biofouling application," Colloids Surf., B 136, 240–247 (2015).

[127]M. Villegas, Y. Zhang, N. Abu Jarad, L. Soleymani, and T. F. Didar, "Liquid-infused surfaces: A review of theory, design, and applications," ACS Nano 13, 8517–8536 (2019).

[128]H. A. Stone, "Ice-phobic surfaces that are wet," ACS Nano 6, 6536–6540 (2012).

[129]S. Anand, A. T. Paxson, R. Dhiman, J. D. Smith, and K. K. Varanasi, "Enhanced condensation on lubricant-impregnated nanotextured surfaces," ACS Nano 6, 10122–10129 (2012).

[130]M. Delmas, M. Monthioux, and T. Ondarçuhu, "Contact angle hysteresis at the nanometer scale," Phys. Rev. Lett. **106**(1–4), 136102 (2011).

[131]C. Semprebon, G. McHale, and H. Kusumaatmaja, "Apparent contact angle and contact angle hysteresis on liquid infused surfaces," Soft Matter **13**, 101–110 (2017).

[132]J. D. Smith, R. Dhiman, S. Anand, E. Reza-Garduno, R. E. Cohen, G. H. McKinley, and K. K. Varanasi, "Droplet mobility on lubricant-impregnated surfaces," Soft Matter **9**, 1772–1780 (2013).

[133]J. D. Smith, R. Dhiman, and K. Varanasi, "Liquid-encapsulating surfaces: Overcoming the limitations of superhydrophobic surfaces for robust non-wetting and anti-icing surfaces," in *APS Division of Fluid Dynamics Meeting Abstracts, APS Meeting Abstracts* (APS, 2011), Vol. 64, p. S4.001.

[134]F. Schellenberger, J. Xie, N. Encinas, A. Hardy, M. Klapper, P. Papadopoulos, H.-J. Butt, and D. Vollmer, "Direct observation of drops on slippery lubricant-infused surfaces," Soft Matter **11**, 7617–7626 (2015).

[135]Q. N. Pham, S. Zhang, K. Montazeri, and Y. Won, "Droplets on slippery lubricant-infused porous surfaces: A macroscale to nanoscale perspective," Langmuir **34**, 14439–14447 (2018).

[136]M. Cao, D. Guo, C. Yu, K. Li, M. Liu, and L. Jiang, "Water-repellent properties of superhydrophobic and lubricant-infused 'slippery' surfaces: A brief study on the functions and applications," ACS Appl. Mater. Interfaces **8**, 3615–3623 (2016).

[137]P. Kim, T.-S. Wong, J. Alvarenga, M. J. Kreder, W. E. Adorno-Martinez, and J. Aizenberg, "Liquid-infused nanostructured surfaces with extreme anti-ice and anti-frost performance," ACS Nano **6**, 6569–6577 (2012).

[138]P. W. Wilson, W. Lu, H. Xu, P. Kim, M. J. Kreder, J. Alvarenga, and J. Aizenberg, "Inhibition of ice nucleation by slippery liquid-infused porous surfaces (SLIPS)," Phys. Chem. Chem. Phys. **15**, 581–585 (2013).

[139]M. Elsharkawy, D. Tortorella, S. Kapatral, and C. M. Megaridis, "Combating frosting with Joule-heated liquid-infused superhydrophobic coatings," Langmuir **32**, 4278–4288 (2016).

[140]P. Zhang, H. Chen, L. Zhang, Y. Zhang, D. Zhang, and L. Jiang, "Stable slippery liquid-infused anti-wetting surface at high temperatures," J. Mater. Chem. A **4**, 12212–12220 (2016).

[141]B. R. Solomon, K. S. Khalil, and K. K. Varanasi, "Drag reduction using lubricant-impregnated surfaces in viscous laminar flow," Langmuir **30**, 10970–10976 (2014).

[142]A. A. Hemeda and H. V. Tafreshi, "Liquid–infused surfaces with trapped air (LISTA) for drag force reduction," Langmuir **32**, 2955–2962 (2016).

[143]M. K. Fu, I. Arenas, S. Leonardi, and M. Hultmark, "Liquid-infused surfaces as a passive method of turbulent drag reduction," J. Fluid Mech. **824**, 688–700 (2017).

[144]A. Lafuma and D. Quéré, "Slippery pre-suffused surfaces," Europhys. Lett. **96**, 56001 (2011).

[145]D. Zhang, Y. Xia, X. Chen, S. Shi, and L. Lei, "PDMS-infused poly(high internal phase emulsion) templates for the construction of slippery liquid-infused porous surfaces with self-cleaning and self-repairing properties," Langmuir **35**, 8276–8284 (2019).

[146]Y. Wang, W. Zhao, W. Wu, C. Wang, X. Wu, and Q. Xue, "Fabricating bionic ultraslippery surface on titanium alloys with excellent fouling-resistant performance," ACS Appl. Bio Mater. **2**, 155–162 (2019).

[147]S. Zouaghi, T. Six, S. Bellayer, S. Moradi, S. G. Hatzikiriakos, T. Dargent, V. Thomy, Y. Coffinier, C. André, G. Delaplace, and M. Jimenez, "Antifouling biomimetic liquid-infused stainless steel: Application to dairy industrial processing," ACS Appl. Mater. Interfaces **9**, 26565–26573 (2017).

[148]H. Li, M. Yan, and W. Zhao, "Designing a MOF-based slippery lubricant-infused porous surface with dual functional anti-fouling strategy," J. Colloid Interface Sci. **607**, 1424–1435 (2022).

[149]H. Pakzad, A. Nouri-Borujerdi, and A. Moosavi, "Drag reduction ability of slippery liquid-infused surfaces: A review," Prog. Org. Coat. **170**, 106970 (2022).

[150]A. C. Glavan, R. V. Martinez, A. B. Subramaniam, H. J. Yoon, R. M. D. Nunes, H. Lange, M. M. Thuo, and G. M. Whitesides, "Omniphobic 'R^F paper' produced by silanization of paper with fluoroalkyltrichlorosilanes," Adv. Funct. Mater. **24**, 60–70 (2014).

[151]D. C. Leslie, A. Waterhouse, J. B. Berthet, T. M. Valentin, A. L. Watters, A. Jain, P. Kim, B. D. Hatton, A. Nedder, K. Donovan, E. H. Super, C. Howell, C. P. Johnson, T. L. Vu, D. E. Bolgen, S. Rifai, A. R. Hansen, M. Aizenberg, M. Super, J. Aizenberg, and D. E. Ingber, "A bioinspired omniphobic surface coating on medical devices prevents thrombosis and biofouling," Nat. Biotechnol. **32**, 1134–1140 (2014).

[152]G. Mackie, L. Gao, S. Yau, D. C. Leslie, and A. Waterhouse, "Clinical potential of immobilized liquid interfaces: Perspectives on biological interactions," Trends Biotechnol. **37**, 268–280 (2019).

[153]A. Tuteja, W. Choi, J. M. Mabry, G. H. McKinley, and R. E. Cohen, "Robust omniphobic surfaces," Proc. Natl. Acad. Sci. U. S. A. **105**, 18200–18205 (2008).

[154]I. Okada and S. Shiratori, "High-transparency, self-standable gel-slips fabricated by a facile nanoscale phase separation," ACS Appl. Mater. Interfaces **6**, 1502–1508 (2014).

[155]W. Ma, Y. Higaki, H. Otsuka, and A. Takahara, "Perfluoropolyether-infused nano-texture: A versatile approach to omniphobic coatings with low hysteresis and high transparency," Chem. Commun. **49**, 597–599 (2013).

[156]B. S. Yilbas, A. Al-Sharafi, and H. Ali, "Chapter 2: Wetting characteristics of surfaces," in *Self-Cleaning of Surfaces and Water Droplet Mobility*, edited by B. S. Yilbas, A. Al-Sharafi, and H. Ali (Elsevier, 2019), pp. 11–44.

[157]A. K. Epstein, T.-S. Wong, R. A. Belisle, E. M. Boggs, and J. Aizenberg, "Liquid-infused structured surfaces with exceptional anti-biofouling performance," Proc. Natl. Acad. Sci. U. S. A. **109**, 13182–13187 (2012).

[158]H. Bazyar, L. Xu, H. J. de Vries, S. Porada, and R. G. H. Lammertink, "Application of liquid-infused membranes to mitigate biofouling," Environ. Sci.: Water Res. Technol. **7**, 68–77 (2021).

[159]S. Basu, B. M. Hanh, J. Q. Isaiah Chua, D. Daniel, M. H. Ismail, M. Marchioro, S. Amini, S. A. Rice, and A. Miserez, "Green biolubricant infused slippery surfaces to combat marine biofouling," J. Colloid Interface Sci. **568**, 185–197 (2020).

[160]Y. Huang, B. B. Stogin, N. Sun, J. Wang, S. Yang, and T. S. Wong, "A switchable cross-species liquid repellent surface," Adv. Mater. **29**, 1604641 (2017).

[161]W. Gao, J. Wang, X. Zhang, L. Sun, Y. Chen, and Y. Zhao, "Electric-tunable wettability on a paraffin-infused slippery pattern surface," Chem. Eng. J. **381**, 122612 (2020).

[162]S. Wang, K. Liu, X. Yao, and L. Jiang, "Bioinspired surfaces with superwettability: New insight on theory, design, and applications," Chem. Rev. **115**, 8230–8293 (2015).

[163]C. Howell, T. L. Vu, C. P. Johnson, X. Hou, O. Ahanotu, J. Alvarenga, D. C. Leslie, O. Uzun, A. Waterhouse, P. Kim, M. Super, M. Aizenberg, D. E. Ingber, and J. Aizenberg, "Stability of surface-immobilized lubricant interfaces under flow," Chem. Mater. **27**, 1792–1800 (2015).

[164]P. Kim, M. J. Kreder, J. Alvarenga, and J. Aizenberg, "Hierarchical or not? Effect of the length scale and hierarchy of the surface roughness on omniphobicity of lubricant-infused substrates," Nano Lett. **13**, 1793–1799 (2013).

[165]P.-G. de Gennes, F. Brochard-Wyart, and D. Quéré, "Capillarity: Deformable interfaces," in *Capillarity and Wetting Phenomena: Drops, Bubbles, Pearls, Waves* (Springer, New York, 2004), pp. 1–31.

[166]N. R. Geraldi, J. H. Guan, L. E. Dodd, P. Maiello, B. B. Xu, D. Wood, M. I. Newton, G. G. Wells, and G. McHale, "Double-sided slippery liquid-infused porous materials using conformable mesh," Sci. Rep. **9**, 13280 (2019).

[167]X. Hou, Y. Hu, A. Grinthal, M. Khan, and J. Aizenberg, "Liquid-based gating mechanism with tunable multiphase selectivity and antifouling behaviour," Nature **519**, 70–73 (2015).

[168]R. Xiao, N. Miljkovic, R. Enright, and E. N. Wang, "Immersion condensation on oil-infused heterogeneous surfaces for enhanced heat transfer," Sci. Rep. **3**, 1988 (2009).

[169]K. Rykaczewski, S. Anand, S. B. Subramanyam, and K. K. Varanasi, "Mechanism of frost formation on lubricant-impregnated surfaces," Langmuir **29**, 5230–5238 (2013).

[170]G. Han, T.-B. Nguyen, S. Park, Y. Jung, J. Lee, and H. Lim, "Moth-eye mimicking solid slippery glass surface with icephobicity, transparency, and self-healing," ACS Nano **14**, 10198–10209 (2020).

[171]R. Gulfam, D. Orejon, C.-H. Choi, and P. Zhang, "Phase-change slippery liquid-infused porous surfaces with thermo-responsive wetting and shedding states," ACS Appl. Mater. Interfaces **12**, 34306–34316 (2020).

[172]B. Pokroy, A. K. Epstein, M. C. M. Persson-Gulda, and J. Aizenberg, "Fabrication of bioinspired actuated nanostructures with arbitrary geometry and stiffness," Adv. Mater. **21**, 463–469 (2009).

[173] R. Sharma, S. S. Das, U. U. Ghosh, S. Dasgupta, and S. Chakraborty, "Pitcher plant inspired biomimetic liquid infused slippery surface using taro leaf," arXiv:1812.10368.

[174] J. Chung, H. Cho, H. Yong, D. Heo, Y. S. Rim, and S. Lee, "Versatile surface for solid–solid/liquid–solid triboelectric nanogenerator based on fluorocarbon liquid infused surfaces," Sci. Technol. Adv. Mater. **21**, 139–146 (2020).

[175] J. Yang, H. Song, H. Ji, and B. Chen, "Slippery lubricant-infused textured aluminum surfaces," J. Adhes. Sci. Technol. **28**, 1949–1957 (2014).

[176] Q. Ma, W. Wang, and G. Dong, "Facile fabrication of biomimetic liquid-infused slippery surface on carbon steel and its self-cleaning, anti-corrosion, anti-frosting and tribological properties," Colloids Surf., A **577**, 17–26 (2019).

[177] X. Fang, Y. Liu, S. Lei, and J. ou, "Slippery liquid-infused porous surface based on MOFs with excellent stability," Chem. Phys. Lett. **771**, 138470 (2021).

[178] P. Kim, W. E. Adorno-Martinez, M. Khan, and J. Aizenberg, "Enriching libraries of high-aspect-ratio micro- or nanostructures by rapid, low-cost, benchtop nanofabrication," Nat. Protoc. **7**, 311–327 (2012).

[179] P. Kim, A. K. Epstein, M. Khan, L. D. Zarzar, D. J. Lipomi, G. M. Whitesides, and J. Aizenberg, "Structural transformation by electrodeposition on patterned substrates (STEPS): A new versatile nanofabrication method," Nano Lett. **12**, 527–533 (2012).

[180] Y. Long, X. Yin, P. Mu, Q. Wang, J. Hu, and J. Li, "Slippery liquid-infused porous surface (SLIPS) with superior liquid repellency, anti-corrosion, anti-icing and intensified durability for protecting substrates," Chem. Eng. J. **401**, 126137 (2020).

[181] A. B. Tesler, L. H. Prado, M. M. Khusniyarov, I. Thievessen, A. Mazare, L. Fischer, S. Virtanen, W. H. Goldmann, and P. Schmuki, "A one-pot universal approach to fabricate lubricant-infused slippery surfaces on solid substrates," Adv. Funct. Mater. **31**, 2101090 (2021).

[182] X. Jing and Z. Guo, "Fabrication of biocompatible super stable lubricant-immobilized slippery surfaces by grafting a polydimethylsiloxane brush: Excellent boiling water resistance, hot liquid repellency and long-term slippery stability," Nanoscale **11**, 8870–8881 (2019).

[183] L. Chen, S. Park, J. Yoo, H. Hwang, H. Kim, J. Lee, J. Hong, and S. Wooh, "One-step fabrication of universal slippery lubricated surfaces," Adv. Mater. Interfaces **7**, 2000305 (2020).

[184] S. Chiera, C. Bittner, and N. Vogel, "Substrate-independent design of liquid-infused slippery surfaces via mussel-inspired chemistry," Adv. Mater. Interfaces **8**, 2100156 (2021).

[185] H. Bazyar, S. Javadpour, and R. G. H. Lammertink, "On the gating mechanism of slippery liquid infused porous membranes," Adv. Mater. Interfaces **3**, 1600025 (2016).

[186] H. Bazyar, P. Lv, J. A. Wood, S. Porada, D. Lohse, and R. G. H. Lammertink, "Liquid–liquid displacement in slippery liquid-infused membranes (SLIMS)," Soft Matter **14**, 1780–1788 (2018).

[187] H. Bazyar, N. van de Beek, and R. G. H. Lammertink, "Liquid-infused membranes with oil-in-water emulsions," Langmuir **35**, 9513–9520 (2019).

[188] S. Wang, Y. Zhang, Y. Han, Y. Hou, Y. Fan, and X. Hou, "Design of porous membranes by liquid gating technology," Acc. Mater. Res. **2**, 407–419 (2021).

[189] M. Ulbricht, "Advanced functional polymer membranes," Polymer **47**, 2217–2262 (2006).

[190] S. Darvishmanesh, X. Qian, and S. R. Wickramasinghe, "Responsive membranes for advanced separations," Curr. Opin. Chem. Eng. **8**, 98–104 (2015), part of Special Issue: Nanotechnology Separation Engineering.

[191] X. Hou, "Smart gating multi-scale pore/channel-based membranes," Adv. Mater. **28**, 7049–7064 (2016).

[192] L.-Y. Chu, "pH-responsive gating membrane systems with pumping effects," Smart Membrane Materials and Systems: From Flat Membranes to Microcapsule Membranes (Springer, Berlin, Heidelberg, 2011), pp. 169–184.

[193] J. D. Willott, W. M. Nielen, and W. M. de Vos, "Stimuli-responsive membranes through sustainable aqueous phase separation," ACS Appl. Polym. Mater. **2**, 659–667 (2020).

[194] L.-Y. Chu, "Thermo-responsive gating membranes: Design, microstructures and performances," in Smart Membrane Materials and Systems: From Flat Membranes to Microcapsule Membranes (Springer, Berlin, Heidelberg, 2011), pp. 19–68.

[195] Y. Ding, G. Panzarasa, S. Stucki, I. Burgert, and T. Keplinger, "Thermo-responsive smart gating wood membranes," ACS Sustainable Chem. Eng. **10**, 5517–5525 (2022).

[196] M. K. Purkait, M. K. Sinha, P. Mondal, and R. Singh, "Chapter 8: Ultrasound-responsive membranes," in Stimuli Responsive Polymeric Membranes, Interface Science and Technology Vol. 25, edited by M. K. Purkait, M. K. Sinha, P. Mondal, and R. Singh (Elsevier, 2018), pp. 221–237.

[197] Y. Liu, C. M. Chow, K. R. Phillips, M. Wang, S. Voskian, and T. A. Hatton, "Electrochemically mediated gating membrane with dynamically controllable gas transport," Sci. Adv. **6**, eabc1741 (2020).

[198] Z. Zhang, L. Wen, and L. Jiang, "Bioinspired smart asymmetric nanochannel membranes," Chem. Soc. Rev. **47**, 322–356 (2018).

[199] Y.-C. Liu, L.-H. Yeh, M.-J. Zheng, and K. C.-W Wu, "Highly selective and high-performance osmotic power generators in subnanochannel membranes enabled by metal-organic frameworks," Sci. Adv. **7**, eabe9924 (2021).

[200] X. Hou, Bio-Inspired Asymmetric Design and Building of Biomimetic Smart Single Nanochannels, Springer Theses (Springer, 2013).

[201] X. Hou, W. Guo, and L. Jiang, "Biomimetic smart nanopores and nanochannels," Chem. Soc. Rev. **40**, 2385–2401 (2011).

[202] Z. S. Siwy and S. Howorka, "Engineered voltage-responsive nanopores," Chem. Soc. Rev. **39**, 1115–1132 (2010).

[203] A. D. Stroock, V. V. Pagay, M. A. Zwieniecki, and N. Michele Holbrook, "The physicochemical hydrodynamics of vascular plants," Annu. Rev. Fluid Mech. **46**, 615–642 (2014).

[204] R. Zhang, J. Lei, J. Xu, H. Fu, Y. Jing, B. Chen, and X. Hou, "Bioinspired photo-responsive liquid gating membrane," Biomimetics **7**, 47 (2022).

[205] M. D. Johnson, H.-F. Bao, M. N. Helms, X.-J. Chen, Z. Tigue, L. Jain, L. G. Dobbs, and D. C. Eaton, "Functional ion channels in pulmonary alveolar type I cells support a role for type I cells in lung ion transport," Proc. Natl. Acad. Sci. U. S. A. **103**, 4964–4969 (2006).

[206] J. Dzubiella, R. J. Allen, and J.-P. Hansen, "Electric field-controlled water permeation coupled to ion transport through a nanopore," J. Chem. Phys. **120**, 5001–5004 (2004).

[207] Y.-C. Yao, Z. Li, A. J. Gillen, S. Yosinski, M. A. Reed, and A. Noy, "Electrostatic gating of ion transport in carbon nanotube porins: A modeling study," J. Chem. Phys. **154**, 204704 (2021).

[208] A. Sharma, R. Kumar, I. Aier, R. Semwal, P. Tyagi, and P. Varadwaj, "Sense of smell: Structural, functional, mechanistic advancements and challenges in human olfactory research," Curr. Neuropharmacol. **17**, 891–911 (2019).

[209] M. Mulder, "Transport in membranes," in Basic Principles of Membrane Technology (Springer Netherlands, Dordrecht, 1991), pp. 145–197.

[210] R. W. Baker, "Overview of membrane science and technology," in Membrane Technology and Applications (John Wiley & Sons, 2004), Chap. 1, pp. 1–14.

[211] L.-Y. Chu, "Introduction," in Smart Membrane Materials and Systems: From Flat Membranes to Microcapsule Membranes (Springer, Berlin, Heidelberg, 2011), pp. 1–17.

[212] B. E. Logan and M. Elimelech, "Membrane-based processes for sustainable power generation using water," Nature **488**, 313–319 (2012).

[213] M. A. Shannon, P. W. Bohn, M. Elimelech, J. G. Georgiadis, B. J. Mariñas, and A. M. Mayes, "Science and technology for water purification in the coming decades," Nature **452**, 301–310 (2008).

[214] S. K. Sikdar and A. Criscuoli, "Sustainability and how membrane technologies in water treatment can be a contributor," in Sustainable Membrane Technology for Water and Wastewater Treatment, edited by A. Figoli and A. Criscuoli (Springer, Singapore, 2017), pp. 1–21.

[215] Smart Membranes, Smart Materials Series, edited by L.-Y. Chu (The Royal Society of Chemistry, 2019), pp. P001–P426.

[216] R. Ghosh, "Stimuli-responsive membranes for separations," in Functional Biopolymers, edited by M. A. Jafar Mazumder, H. Sheardown, and A. Al-Ahmed (Springer International Publishing, Cham, 2019), pp. 491–508.

[217] T. Meng, R. Xie, Y.-C. Chen, C.-J. Cheng, P.-F. Li, X.-J. Ju, and L.-Y. Chu, "A thermo-responsive affinity membrane with nano-structured pores and grafted poly(N-isopropylacrylamide) surface layer for hydrophobic adsorption," J. Membr. Sci. **349**, 258–267 (2010).

[218] D. Menne, F. Pitsch, J. E. Wong, A. Pich, and M. Wessling, "Temperature-modulated water filtration using microgel-functionalized hollow-fiber membranes," Angew. Chem., Int. Ed. **53**, 5706–5710 (2014).

[219] L.-Y. Chu, T. Yamaguchi, and S. Nakao, "A molecular-recognition microcapsule for environmental stimuli-responsive controlled release," Adv. Mater. **14**, 386–389 (2002).

[220] J. I. Clodt, V. Filiz, S. Rangou, K. Buhr, C. Abetz, D. Höche, J. Hahn, A. Jung, and V. Abetz, "Double stimuli-responsive isoporous membranes via post-modification of pH-sensitive self-assembled diblock copolymer membranes," Adv. Funct. Mater. **23**, 731–738 (2013).

[221] L.-Y. Chu, Y. Li, J.-H. Zhu, and W.-M. Chen, "Negatively thermoresponsive membranes with functional gates driven by zipper-type hydrogen-bonding interactions," Angew. Chem., Int. Ed. **44**, 2124–2127 (2005).

[222] M. Yang, L.-Y. Chu, H.-D. Wang, R. Xie, H. Song, and C. H. Niu, "A thermoresponsive membrane for chiral resolution," Adv. Funct. Mater. **18**, 652–663 (2008).

[223] B. Yang and W. Yang, "Thermo-sensitive switching membranes regulated by pore-covering polymer brushes," J. Membr. Sci. **218**, 247–255 (2003).

[224] L. Wang, H. Zhang, Z. Yang, J. Zhou, L. Wen, L. Li, and L. Jiang, "Fabrication of hydrogel-coated single conical nanochannels exhibiting controllable ion rectification characteristics," Phys. Chem. Chem. Phys. **17**, 6367–6373 (2015).

[225] See https://www.macmillanhighered.com/BrainHoney/Resource/6716/digital_first_content/trunk/test/hillis2e/asset/img_ch5/c05_fig04.html for "A ligand-gated channel protein opens in response to a stimulus," (Macmillan Learning, 2022) (Last accessed, May 2022).

[226] L.-Y. Chu, Y. Li, J.-H. Zhu, H.-D. Wang, and Y.-J. Liang, "Control of pore size and permeability of a glucose-responsive gating membrane for insulin delivery," J. Controlled Release **97**, 43–53 (2004).

[227] J. Ran, L. Wu, Z. Zhang, and T. Xu, "Atom transfer radical polymerization (ATRP): A versatile and forceful tool for functional membranes," Prog. Polym. Sci. **39**, 124–144 (2014).

[228] J. Deng, L. Wang, L. Liu, and W. Yang, "Developments and new applications of UV-induced surface graft polymerizations," Prog. Polym. Sci. **34**, 156–193 (2009).

[229] J. Xue, L. Chen, H. L. Wang, Z. B. Zhang, X. L. Zhu, E. T. Kang, and K. G. Neoh, "Stimuli-responsive multifunctional membranes of controllable morphology from poly(vinylidene fluoride)-*graft*-poly[2-(N,N-dimethylamino)ethyl methacrylate] prepared via atom transfer radical polymerization," Langmuir **24**, 14151–14158 (2008).

[230] F. Luo, R. Xie, Z. Liu, X. J. Ju, W. Wang, S. Lin, and L. Y. Chu, "Smart gating membranes with *in situ* self-assembled responsive nanogels as functional gates," Sci. Rep. **5**, 14708 (2015).

[231] M. Nishizawa, V. P. Menon, and C. R. Martin, "Metal nanotubule membranes with electrochemically switchable ion-transport selectivity," Science **268**, 700–702 (1995).

[232] X. Hou, Y. Liu, H. Dong, F. Yang, L. Li, and L. Jiang, "A pH-gating ionic transport nanodevice: Asymmetric chemical modification of single nanochannels," Adv. Mater. **22**, 2440–2443 (2010).

[233] M. Ali, B. Yameen, R. Neumann, W. Ensinger, W. Knoll, and O. Azzaroni, "Biosensing and supramolecular bioconjugation in single conical polymer nanochannels. Facile incorporation of biorecognition elements into nanoconfined geometries," J. Am. Chem. Soc. **130**, 16351–16357 (2008).

[234] C. Liangyin, X. Rui, and J. Xiaojie, "Stimuli-responsive membranes: Smart tools for controllable mass-transfer and separation processes," Chin. J. Chem. Eng. **19**, 891–903 (2011).

[235] D. Schmaljohann, "Thermo- and pH-responsive polymers in drug delivery," Adv. Drug Delivery Rev. **58**, 1655–1670 (2006), part of Special Issue: 2006 Supplementary Non-Thematic Collection.

[236] Z. Liu, F. Luo, X.-J. Ju, R. Xie, T. Luo, Y.-M. Sun, and L.-Y. Chu, "Positively K$^+$-responsive membranes with functional gates driven by host–guest molecular recognition," Adv. Funct. Mater. **22**, 4742–4750 (2012).

[237] E. G. Kelley, J. N. L. Albert, M. O. Sullivan, and T. H. Epps III, "Stimuli-responsive copolymer solution and surface assemblies for biomedical applications," Chem. Soc. Rev. **42**, 7057–7071 (2013).

[238] L.-Y. Chu, "Glucose-responsive gating membranes," in *Smart Membrane Materials and Systems: From Flat Membranes to Microcapsule Membranes* (Springer, Berlin, Heidelberg, 2011), pp. 197–216.

[239] G. Pasparakis, T. Manouras, P. Argitis, and M. Vamvakaki, "Photodegradable polymers for biotechnological applications," Macromol. Rapid Commun. **33**, 183–198 (2012).

[240] J. Thévenot, H. Oliveira, O. Sandre, and S. Lecommandoux, "Magnetic responsive polymer composite materials," Chem. Soc. Rev. **42**, 7099–7116 (2013).

[241] M. Yazdani, Z. Jia, and J. Chen, "Hydrophobic dewetting in gating and regulation of transmembrane protein ion channels," J. Chem. Phys. **153**, 110901 (2020).

[242] H. G. Schild, "Poly(N-isopropylacrylamide): Experiment, theory and application," Prog. Polym. Sci. **17**, 163–249 (1992).

[243] L.-Y. Chu, T. Niitsuma, T. Yamaguchi, and S.-i. Nakao, "Thermoresponsive transport through porous membranes with grafted PNIPAM gates," AIChE J. **49**, 896–909 (2003).

[244] R. Xie, Y. Li, and L.-Y. Chu, "Preparation of thermo-responsive gating membranes with controllable response temperature," J. Membr. Sci. **289**, 76–85 (2007).

[245] X.-J. Ju, R. Xie, L. Yang, and L.-Y. Chu, "Biodegradable 'intelligent' materials in response to chemical stimuli for biomedical applications," Expert Opin. Ther. Pat. **19**, 683–696 (2009).

[246] J.-B. Qu, L.-Y. Chu, M. Yang, R. Xie, L. Hu, and W.-M. Chen, "A pH-responsive gating membrane system with pumping effects for improved controlled release," Adv. Funct. Mater. **16**, 1865–1872 (2006).

[247] T. Luo, S. Lin, R. Xie, X.-J. Ju, Z. Liu, W. Wang, C.-L. Mou, C. Zhao, Q. Chen, and L.-Y. Chu, "pH-responsive poly(ether sulfone) composite membranes blended with amphiphilic polystyrene-*block*-poly(acrylic acid) copolymers," J. Membr. Sci. **450**, 162–173 (2014).

[248] S. Milster, W. K. Kim, M. Kanduč, and J. Dzubiella, "Tuning the permeability of regular polymeric networks by the cross-link ratio," J. Chem. Phys. **154**, 154902 (2021).

[249] P. S. Laplace, *Traité de Mécanique Céleste, Tome Quatriéme*, Treatise on Celestial Mechanics Tome 4 (Courcier, Paris, France, 1805), pp. 349–417, Supplément au Livre X du Traité de Mécanique Céleste, Sur l'Action Capillaire (Supplement to Book 10 of the Treatise on Celestial Mechanics. On the capillary action).

[250] J. C. Berg, "Fluid interfaces and capillarity," in *An Introduction to Interfaces and Colloids* (World Scientific, 2009), Chap. 2, pp. 23–106.

[251] D. J. Preston, Y. Song, Z. Lu, D. S. Antao, and E. N. Wang, "Design of lubricant infused surfaces," ACS Appl. Mater. Interfaces **9**, 42383–42392 (2017).

[252] Z. Sheng, Z. Zhang, J. Liu, P. Malgaretti, J. Li, S. Wang, W. Lv, R. Zhang, Y. Fan, Y. Zhang, X. Chen, and X. Hou, "Reconfiguring confined magnetic colloids with tunable fluid transport behavior," Natl. Sci. Rev. **8**, nwaa301 (2020).

[253] H. Wang, Y. Fan, Y. Hou, B. Chen, J. Lei, S. Yu, X. Chen, and X. Hou, "Host-guest liquid gating mechanism with specific recognition interface behavior for universal quantitative chemical detection," Nat. Commun. **13**, 1906 (2022).

[254] B. Chen, M. Zhang, Y. Hou, H. Wang, R. Zhang, Y. Fan, X. Chen, and X. Hou, "Energy saving thermal adaptive liquid gating system," Innovation **3**, 100231 (2022).

[255] S. Yu, Y. Jing, Y. Fan, L. Xiong, H. Wang, J. Lei, Y. Zhang, J. Liu, S. Wang, X. Chen, H. Sun, and X. Hou, "Ultrahigh efficient emulsification with drag-reducing liquid gating interfacial behavior," Proc. Natl. Acad. Sci. U. S. A. **119**, e2206462119 (2022).

[256] S. Yu, L. Pan, Y. Zhang, X. Chen, and X. Hou, "Liquid gating technology," Pure Appl. Chem. **93**, 1353–1370 (2021).

[257] Z. Sheng, J. Zhang, J. Liu, Y. Zhang, X. Chen, and X. Hou, "Liquid-based porous membranes," Chem. Soc. Rev. **49**, 7907–7928 (2020).

[258] R. Lenormand, E. Touboul, and C. Zarcone, "Numerical models and experiments on immiscible displacements in porous media," J. Fluid Mech. **189**, 165–187 (1988).

[259] Z. Liu, F. Luo, X.-J. Ju, R. Xie, Y.-M. Sun, W. Wang, and L.-Y. Chu, "Gating membranes for water treatment: Detection and removal of trace Pb^{2+} ions based on molecular recognition and polymer phase transition," J. Mater. Chem. A **1**, 9659–9671 (2013).

[260] S. R. Lewis, S. Datta, M. Gui, E. L. Coker, F. E. Huggins, S. Daunert, L. Bachas, and D. Bhattacharyya, "Reactive nanostructured membranes for water purification," Proc. Natl. Acad. Sci. U. S. A. **108**, 8577–8582 (2011).

[261] W. Sun, J. Liu, H. Chu, and B. Dong, "Pretreatment and membrane hydrophilic modification to reduce membrane fouling," Membranes **3**, 226–241 (2013).

[262]S. J. Zaidi, K. A. Mauritz, and M. K. Hassan, "Membrane surface modification and functionalization," in *Functional Polymers*, edited by M. A. Jafar Mazumder, H. Sheardown, and A. Al-Ahmed (Springer International Publishing, Cham, 2018), pp. 1–26.

[263]Z. Sheng, H. Wang, Y. Tang, M. Wang, L. Huang, L. Min, H. Meng, S. Chen, L. Jiang, and X. Hou, "Liquid gating elastomeric porous system with dynamically controllable gas/liquid transport," Sci. Adv. **4**, eaao6724 (2018).

[264]X. Hou, "Liquid gating membrane," Natl. Sci. Rev. **7**, 9–11 (2019).

[265]W. Liu, M. Wang, Z. Sheng, Y. Zhang, S. Wang, L. Qiao, Y. Hou, M. Zhang, X. Chen, and X. Hou, "Mobile liquid gating membrane system for smart piston and valve applications," Ind. Eng. Chem. Res. **58**, 11976–11984 (2019).

[266]A. B. Tesler, Z. Sheng, W. Lv, Y. Fan, D. Fricke, K.-C. Park, J. Alvarenga, J. Aizenberg, and X. Hou, "Metallic liquid gating membranes," ACS Nano **14**, 2465–2474 (2020).

[267]J. Liu, X. Xu, Y. Lei, M. Zhang, Z. Sheng, H. Wang, M. Cao, J. Zhang, and X. Hou, "Liquid gating meniscus-shaped deformable magnetoelastic membranes with self-driven regulation of gas/liquid release," Adv. Mater. **34**, 2107327 (2022).

[268]Y. Han, Y. Zhang, M. Zhang, B. Chen, X. Chen, and X. Hou, "Photothermally induced liquid gate with navigation control of the fluid transport," Fundam. Res. **1**, 800–806 (2021).

[269]M. M. Pendergast and E. M. V. Hoek, "A review of water treatment membrane nanotechnologies," Energy Environ. Sci. **4**, 1946–1971 (2011).

[270]B. D. McCloskey, H. B. Park, H. Ju, B. W. Rowe, D. J. Miller, and B. D. Freeman, "A bioinspired fouling-resistant surface modification for water purification membranes," J. Membr. Sci. **413-414**, 82–90 (2012).

[271]Y. Zhu, W. Xie, J. Li, T. Xing, and J. Jin, "pH-induced non-fouling membrane for effective separation of oil-in-water emulsion," J. Membr. Sci. **477**, 131–138 (2015).

[272]W. Zhang, N. Liu, Y. Cao, Y. Chen, L. Xu, X. Lin, and L. Feng, "A solvothermal route decorated on different substrates: Controllable separation of an oil/water mixture to a stabilized nanoscale emulsion," Adv. Mater. **27**, 7349–7355 (2015).

[273]X. Gao, L.-P. Xu, Z. Xue, L. Feng, J. Peng, Y. Wen, S. Wang, and X. Zhang, "Dual-scaled porous nitrocellulose membranes with underwater super-oleophobicity for highly efficient oil/water separation," Adv. Mater. **26**, 1771–1775 (2014).

[274]L. Zhang, Z. Zhang, and P. Wang, "Smart surfaces with switchable superoleophilicity and superoleophobicity in aqueous media: Toward controllable oil/water separation," NPG Asia Mater. **4**, e8 (2012).

[275]C. Song and G. C. Rutledge, "Electrospun liquid-infused membranes for emulsified oil/water separation," Langmuir **38**, 2301–2313 (2022).

[276]Y. Wang, J. Di, L. Wang, X. Li, N. Wang, B. Wang, Y. Tian, L. Jiang, and J. Yu, "Infused-liquid-switchable porous nanofibrous membranes for multiphase liquid separation," Nat. Commun. **8**(1), 575 (2017).

[277]J. C. Overton, A. Weigang, and C. Howell, "Passive flux recovery in protein-fouled liquid-gated membranes," J. Membr. Sci. **539**, 257–262 (2017).

[278]M. Stoller, D. Baiocco, A. Cicci, and M. Bravi, "Description of the biofouling phenomena affecting membranes by the boundary flux concept," Chem. Eng. Trans. **49**, 589–594 (2016).

[279]R. Komlenic, "Rethinking the causes of membrane biofouling," Filtr. Sep. **47**, 26–28 (2010).

[280]R. M. Shah, A. Cihanoğlu, J. Hardcastle, C. Howell, and J. D. Schiffman, "Liquid-infused membranes exhibit stable flux and fouling resistance," ACS Appl. Mater. Interfaces **14**, 6148–6156 (2022).

[281]Y. Fan, Z. Sheng, J. Chen, H. Pan, B. Chen, F. Wu, S. Wang, X. Chen, and X. Hou, "Visual chemical detection mechanism by a liquid gating system with dipole-induced interfacial molecular reconfiguration," Agnew. Chem. **131**, 4007–4011 (2019).

[282]B. Chen, R. Zhang, Y. Hou, J. Zhang, S. Chen, Y. Han, X. Chen, and X. Hou, "Light-responsive and corrosion-resistant gas valve with non-thermal effective liquid-gating positional flow," Light: Sci. Appl. **10**, 127 (2021).

[283]J. Lei, Y. Hou, H. Wang, Y. Fan, Y. Zhang, B. Chen, S. Yu, and X. Hou, "Carbon dioxide chemically responsive switchable gas valves with protonation-induced liquid gating self-adaptive systems," Angew. Chem., Int. Ed. **61**, e202201109 (2022).

[284]C. Wang, S. Wang, H. Pan, L. Min, H. Zheng, H. Zhu, G. Liu, W. Yang, X. Chen, and X. Hou, "Bioinspired liquid gating membrane-based catheter with anticoagulation and positionally drug release properties," Sci. Adv. **6**, eabb4700 (2020).

[285]M. Khayet and T. Matsuura, "Chapter 3: Formation of flat sheet phase inversion MD membranes," in *Membrane Distillation*, edited by M. Khayet and T. Matsuura (Elsevier, Amsterdam, 2011), pp. 41–58.

[286]M. E. Warkiani, A. A. S. Bhagat, B. L. Khoo, J. Han, C. T. Lim, H. Q. Gong, and A. G. Fane, "Isoporous micro/nanoengineered membranes," ACS Nano **7**, 1882–1904 (2013).

[287]L. Pu, M. Zhu, X. Shen, S. Wu, W. Wei, and S. Li, "Stomata-inspired smart bilayer catalyst with the dual-responsive ability, capable of single/tandem catalysis," Polymer **234**, 124238 (2021).